

NSP 2018 INTERNATIONAL WORKSHOP
AND SCHOOL
**Nanostructures
for Photonics**

Abstracts

May 7–12 • Saint Petersburg • Russia

Organizers:

ITMO University
Fund for Laser Physics
EU Marie Curie Initial Training Network «INDEED»

Co-chairs:

Vladimir Dubrovskii
Frank Glas

Sponsors:

ITMO University
Ministry of Education and Research of the Russian Federation
EU Marie Skłodowska-Curie ITN «INDEED»
Russian Foundation for Basic Research

Contents

Tuesday, May 8

i-Tue1	<i>J. Tersoff</i> , L. Camilli, J.H. Jørgensen, A.C. Stoot, R. Balog, A. Cassidy, J.T. Sadowski, P. Bøggild, L. Hornekær Self-assembly of ordered graphene nanodot arrays within a 2D BCN alloy	6
i-Tue2	<i>J. Johansson</i> , E.D. Leshchenko, and M. Ghasemi Understanding the composition of VLS grown ternary III-V nanowires	7
i-Tue3	<i>A.E. Romanov</i> Dislocations in photonic heterostructures	8
i-Tue6	<i>A. Fontcuberta i Morral</i> Novel compound semiconductor nanostructures for photonics	9

Wednesday, May 9

i-Wed1	<i>P.C. McIntyre</i> Group IV nanowire structure, luminescence and carrier dynamics	10
i-Wed2	<i>M. Tchernycheva</i> , N. Guan, M. Morassi, L. Mancini, C. Barbier, N. Amador, A. Kapoor, J. Eymery, C. Durand, L. Lu, N. Gogneau, A. Madouri, F.H. Julien, L. Largeau, J.-C. Harmand Nitride nanowires on graphene for flexible optoelectronics	11
i-Wed4	<i>Y. Arakawa</i> Advances of quantum dots for lasers and single photon sources	12
i-Wed6	<i>R.R. LaPierre</i> III-V materials development for nanowire photodetectors and photovoltaics	13
i-Wed7	<i>M. De Luca</i> Optical and phononic properties of nanowires on demand	14
i-Wed8	<i>G.E. Cirlin</i> , N. Akopian Hybrid quantum dot in a nanowire systems	15
i-Wed9	<i>Z.R. Zytkiewicz</i> Self-assembled formation of GaN nanowires on amorphous substrates	16
i-Wed10	<i>V.G. Dubrovskii</i> , F. Glas, G. Patriarche, F. Panciera, J.-C. Harmand “Stopping” effect and its role in oscillations of truncation in III-V nanowires	17
i-Wed12	<i>A.M. Korsunsky</i> , I.P. Dolbnya, T. Sui, J.J. Baumberg, Q. Zhao Small angle X-ray scattering of a stretchable photonic crystal	18

Friday, May 11

i-Fri4	<i>E. Joselevich</i> Guided nanowire optoelectronics	19
i-Fri5	<i>T. Hakkarainen</i> , E. Koivusalo, M.R. Piton, E. Petronijevic, G. Leahu, A. Belardini, M. Centini, C. Sibilia, V.G. Dubrovskii, M. Guina Self-catalyzed molecular beam epitaxy of GaAs nanowires for photonic applications	20
i-Fri6	<i>R. Feidenhans'l</i> New opportunities at European XFEL	22
i-Fri7	<i>P. Roca i Cabarrocas</i> Low temperature plasma deposition processes: from amorphous silicon to epitaxial growth and nanowires	23
i-Fri9	<i>M.O. Nestoklon</i> Intervalley mixing due to interfaces in semiconductor nanostructures	24

Poster Session, Tuesday, May 8

p-Tue1	<i>N. Amador</i> , N. Guan, X. Dai, H. Zhang, V. Piazza, A. Kapoor, C. Bougerol, L. Mancini, F.H. Julien, H. Chalermchai, A. Cattoni, S. Collin, F. Oehler, J.-C. Harmand, J. Eymery, C. Durand and M. Tchernycheva Flexible optoelectronic devices based on III-nitride nanowires	25
p-Tue2	<i>M. Apollo</i> , J. Major, W. Stepniowski, M. Tormen and K. Durose Cadmium telluride nanowire growth for photovoltaic application	27
p-Tue5	<i>M. Friedl</i> , A. Balgarkashi, L. Francaviglia, S. Marti-Sanchez, L. Güniat, W. Kim, V.G. Dubrovskii, J. Arbiol, A. Fontcuberta i Morral InGaAs nanowires grown on GaAs nanomembranes by MBE	28
p-Tue6	<i>A. Galan</i> , A.J. Gallant, A. Fontcuberta i Morral, F. Alkhalil, D.A. Zeze, D. Atkinson Large area single crystal ZnO nanowires grown on ALD seed layers	29

p-Tue7	Z.M. Lashkami, E. Gholami Lasers, sources of single photons and entangled photon pairs based on quantum dot in nanowire system	31
p-Tue9	V. Kaliteevskii, L. Chechurin Nanowires as the object of patenting: landscaping	32
p-Tue10	A.K. Sivan, L. Di Mario, S. Rubini and F. Martelli Stationary and transient optical measurements in semiconductor nanowires	33
p-Tue12	W. Kim, V.G. Dubrovskii, Vukajlovic-Plestina, G. Tuñuicuöglu, L. Francaviglia, D. Mikulik, E. Stutz, L. Guñiat, H. Potts, M. Friedl, J.-B. Leran and A. Fontcuberta i Morral Ordered GaAs nanowire arrays on silicon and dopant incorporation studies	34
p-Tue13	E. Koivusalo, T. Hakkarainen, M. Guina Turning the growth direction of GaAs NWs during self-catalyzed MBE	35
p-Tue15	E.D. Leshchenko, M. Ghasemi, V.G. Dubrovskii, J. Johansson Nucleation limited composition of ternary nanowires	36
p-Tue17	N. Peric, A. Diaz-Alvarez, T. Xu, M. Schnedler, I. Lefebvre, G. Patriarche, J.P. Nys, S.R. Plissard, P. Caroff, M. Berthe, H. Eisele, R.E. Dunin-Borkowski, Ph. Ebert, B. Grandidier Controlling the surface morphology of III-V semiconductor nanowires	37
p-Tue18	A. Pishchagin, F. Glas, J.-C. Harmand, F. Oehler Growth of advanced functional heterostructures in III-V nanowires	38
p-Tue19	R.R. Reznik, K.P. Kotlyar, I.P. Soshnikov, E.V. Nikitina, S.A. Kukushkin, A.V. Osipov and G.E. Cirlin MBE growth and optical properties of GaN, InN and III-V nanowires on SiC/Si(111) hybrid substrate	39
p-Tue20	M.R. Piton, E. Koivusalo, S. Suomalainen, T. Hakkarainen, S. Souto, H.V.A. Galeti, D. Lupo, A.D. Rodrigues, Y.G. Gobato and M. Guina Structural and transport properties of Be-doped self-catalysed GaAs nanowires grown by molecular beam epitaxy	40
p-Tue21	P.R. Martínez, B. Horrocks, A. Houlton Preparing nanomaterials based on metals and DNA	42
p-Tue23	E. Vissol-Gaudin, A. Kotsialos, C. Pearson, C. Groves, M.C. Petty and D.A. Zeze Using carbon-nanotube classifiers to diagnose diseases	44
p-Tue24	D. Paige Wilson, R.R. LaPierre Increasing nanowire diameters for solar cell applications	46
p-Tue25	Y. Berdnikov, N.V. Sibirev Model for growth modes of PA MBE GaN nanowires	47
p-Tue26	A.A. Koryakin, S.A. Kukushkin, N.V. Sibirev Vapor-solid-solid growth mechanism of Au-catalyzed III-V nanowires	48
p-Tue27	A.S. Sokolovskii, V.G. Dubrovskii Au droplet stability in InAs nanowires growth	49
	Author Index	50
	List of Participants	51

Self-assembly of ordered graphene nanodot arrays within a 2D BCN alloy

J. Tersoff, L. Camilli, J.H. Jørgensen, A.C. Stoot, R. Balog, A. Cassidy, J.T. Sadowski, P. Bøggild,
L. Hornekær

IBM T.J. Watson Research Center

The ability to fabricate nanoscale domains of uniform size in two-dimensional (2D) materials could potentially enable new applications in nanoelectronics and the development of innovative metamaterials. In particular, uniform-size semiconducting quantum dots have potential applications in nanophotonics. However, it has proven extremely difficult to achieve even minimal control over the growth of 2D lateral heterostructures at such extreme dimensions.

Recently Camilli *et al.* [1] found that ordered arrays of graphene nano-domains (quantum dots) can form spontaneously during the growth of 2D boron–carbon–nitrogen (BCN) alloy. These dots exhibit a strikingly uniform size of 1.6 ± 0.2 nm, as well as strong ordering. Moreover, the array periodicity can be tuned by adjusting the growth conditions. The graphene quantum dots are epitaxially embedded within the 2D BCN alloy, so the whole system forms a continuous atomic sheet.

We believe that the behavior here cannot be explained by familiar mechanisms of domain self-organization. Instead we propose that this system is controlled by the moiré-modulated interactions with the substrate. We develop a simple model incorporating dot-boundary energy, the moiré-modulated substrate interaction, and the expected long-range repulsion between dots. The model successfully describes the observed behavior, and gives insight into the energetics.

Based on previous calculations of the band gap of graphene dots, we expect that the dots in this new 2D material are semiconducting. The system therefore corresponds to an ordered composite of uniform semiconducting graphene quantum dots, laterally integrated within a larger-bandgap matrix. This promises novel electronic and photonic properties, with a variety of potential device applications.

References

- [1] L. Camilli, J.H. Jørgensen, J. Tersoff, *et al.*, *Nature Comm.* **8**, 47 (2017).

Understanding the composition of VLS grown ternary III-V nanowires

J. Johansson¹, E.D. Leshchenko¹, and M. Ghasemi²

¹ Solid State Physics and NanoLund, Lund University, Box 118, 221 00 Lund, Sweden

² Persian Gulf University, Physics Department, Box 7513613817 Booshehr, Iran

Bandgap engineering is an important enabling technology for electronics and optoelectronics applications of III-V semiconductor nanowires. The most straightforward approach to bandgap engineering in nanowires is composition control in ternary nanowires, both for radial and longitudinal growth. There are a few experimental investigations with the aim to control the composition in ternary nanowires and one of the most investigated systems is InGaAs. Other experimentally investigated ternary nanowire systems are InGaSb, AlGaAs, InAsSb, and GaAsSb. Even if there are some theoretical efforts to relate the composition of the solid nanowire to the composition of the vapor phase, there is limited understanding of how the composition of the seed particle influences the composition of the nanowire.

In order to understand composition control in ternary nanowire systems and draw relevant conclusions, it is of highest importance to have access to realistic and thermodynamically assessed chemical potentials for all involved phases. The modern way to assess thermodynamic systems is known as CALPHAD (calculation of phase diagrams) [1]. In this context assess means to fit experimental or calculated thermodynamic data to specified models for the Gibbs free energies for all the phases. This procedure results in a thermodynamic database from which phase diagrams and other properties of interest can be calculated. In our case of composition control, the chemical potentials of the solid nanowire phase and the liquid metal phase are the most interesting properties. Before going into any details of composition control, we will give a brief introduction to the CALPHAD method.

The aim of the presentation is to explain how the nanowire composition during longitudinal, metal particle-seeded growth depends on the composition of the seed alloy particle. We have previously discussed the composition of $\text{In}_x\text{Ga}_{1-x}\text{As}$ nanowires in the nucleation limited regime, approximating the composition of the solid material with the composition of the critical nucleus [2]. Here we follow up on our previous work and demonstrate that analytically calculated composition curves can be calculated for a wide range of nanowire materials [3] provided that the chemical potentials are known.

Moreover, we propose a model for the kinetically limited composition of metal particle-seeded ternary III-V nanowires. The model is based on diffusion limited growth of supercritical nuclei within two-component nucleation theory. We derive the model for the general case and then we discuss it in terms of InGaAs nanowire growth. Applying the model to gold-seeded and self-seeded growth of InGaAs we are able to explain the experimentally obtained features related to nanowire compositions, including the attainability of compositions within the miscibility gap, see Fig. 1. Based on our calculations and comparisons with experiments, we recommend that self-seeded growth with composition control should be carried out at low temperature, even if this is reported to be technically chal-

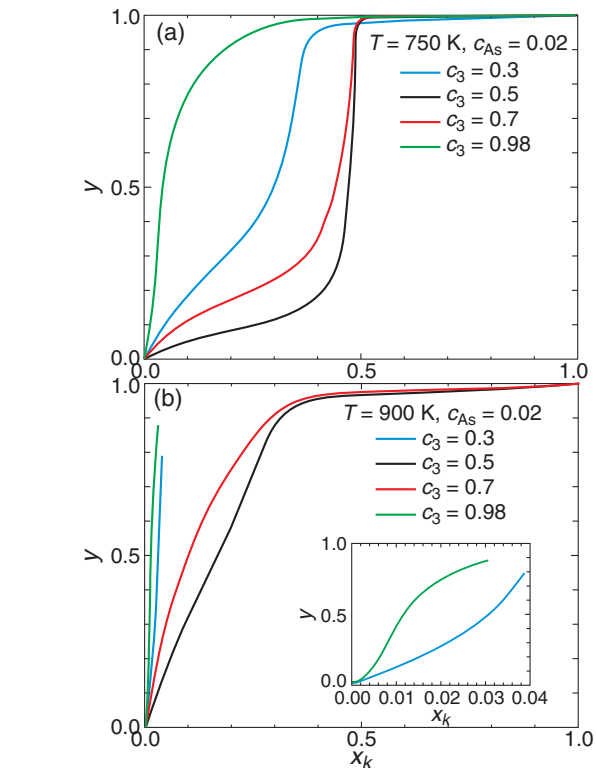


Fig. 1. The steady state InAs composition of the supercritical nucleus, x_k , as a function of the In fraction of the group III content, y , with varying total group III molar fraction, c_3 , calculated for (a) $T = 750$ K and (b) $T = 900$ K. The inset shows a zoomed view of the $c_3 = 0.3$ and $c_3 = 0.98$ curves. For y higher than approximately 0.8–0.9 for these cases, the system becomes undersaturated.

lenging [4]. On the other hand, for gold-seeded growth with composition control over the full range, we recommend growth at high temperature. In addition, by directly comparing with experiments we conclude that approximately 2% arsenic in the alloy particle during self-seeded growth of InGaAs is a realistic assumption [5].

References

- [1] H.L. Lukas, S.G. Fries, B. Sundman, Computational thermodynamics: the Calphad method, Cambridge University press (2007).
- [2] J. Johansson, M. Ghasemi, *Crystal Growth & Design* **17**, 1630 (2017).
- [3] E. Leshchenko, M. Ghasemi, V. G. Dubrovskii, J. Johansson, *CrystEngComm* **20**, 1649 (2018).
- [4] M. Heiss, B. Ketterer, E. Uccelli, *et al*, *Nanotechnology* **22**, 195601 (2011).
- [5] J. Johansson, M.Ghasemi, *Phys Rev Materials* **1**, 040401(R) (2017).

Dislocations in photonic heterostructures

A.E. Romanov

ITMO University, Kronversky pr. 49, 197101 St Petersburg, Russia

The relaxation of mechanical stresses in lattice-mismatched photonic heterostructures usually occurs via misfit dislocation (MD) formation at interfaces and are accompanied by the generation of high density of threading dislocations (TDs) in the bulk of the material. Whereas MDs can be considered as equilibrium defects for initially stressed heterostructures, TDs are essentially nonequilibrium defects generated due kinetic reasons. Threading dislocations are deleterious for wide variety of modern photonic devices including light-emitting diodes (LEDs) and laser diodes (LDs). Relaxation in stressed epitaxial layers also gives rise to cracking, change of surface morphology, and bowing of the heterostructures during growth and/or after processing.

In recent two decades, there have been substantial experimental and theoretical efforts to understand stress relaxation in semiconductor photonic heterostructures and to reduce TD densities in active regions of photonic devices based on various semiconductor compound heterostructures. In present talk, advanced approaches to modelling MD formation and TD reduction are considered and a number of successful models are discussed in details [1–10].

Cross-hatch surface morphology widely observed in photonic heterostructures is directly related to strain relaxation via TD glide, which results in both formation of surface steps and MDs. This mechanism operates for materials with inclined slip planes, i.e. FCC layers grown in (001) orientation. Another specific stress relaxation mechanism operates via the inclination of TDs, which were initially normal to the film surface. This mechanism works, for example, for III-nitride layers with wurtzite crystal structure grown in (0001) orientation. For semipolar growth of III-nitride photonic heterostructures stress relaxation via dislocation glide either in basal (0001)/ $\langle 11\bar{2}0 \rangle$ or prismatic $\{10\bar{1}0\}$ / $\langle 11\bar{2}0 \rangle$ slip systems becomes preferential; in this case the shear stresses driving the dislocations on inclined basal or prismatic planes do not vanish.

In analysing TD density reduction two fundamental issues are identified: (i) relative dislocation motion and (ii) reactions between dislocations. One type of TD motion is specific to non-relaxed (i.e. strained layers) when a mobile TD produces a new MD diminishing in such a way the global misfit stress in the film. The other type of TD effective motion takes place even in relaxed buffer layers when the point, at which an inclined TD meets the layer surface, laterally displaces when the layer growth proceeds. For the reduction of dislocation density, the reactions of annihilation and fusion among TDs are important. To study quantitatively the evolution of TD ensemble the ‘reaction kinetics’ equations for TD and MD densities were derived and analysed both analytically and numerically.

The modelling results on dislocation behaviour in photonic heterostructures are supported by extensive experimental data on stress relaxation in typical film/substrate systems: epitaxial (001) heterostructures of III-V compounds and III-nitride heterostructures grown both in (0001) polar and semipolar orientations.

References

- [1] A.E. Romanov *et al*, *APL* **69** 3342 (1996).
- [2] J.S. Speck *et al*, *JAP* **80** 3808 (1996).
- [3] A.E. Romanov *et al*, *JAP* **85** 182 (1999).
- [4] A.E. Romanov and J.S. Speck, *APL* **83** 2569 (2003).
- [5] A.M. Andrews *et al*, *JAP* **95** 6032 (2004).
- [6] A.E. Romanov *et al*, *JAP* **100** 023522 (2006).
- [7] E.C. Young *et al*, *APL* **96** 041913 (2010).
- [8] A.E. Romanov *et al*, *JAP* **109** 103552 (2011).
- [9] M.T. Hardy *et al*, *APL* **100** 202103 (2012).
- [10] A.M. Smirnov *et al*, *APL Materials* **4** 016105 (2016).

Novel compound semiconductor nanostructures for photonics

A. Fontcuberta i Morral

Laboratory of Semiconductor Materials, Institute of Materials, EPFL, 1015 Lausanne, Switzerland

Nanowires are filamentary crystals with a tailored diameter ranging from few to ~ 100 nm. The reduced dimensions and longitudinal morphology of these nanowires results in interesting optical and electrical properties and provides a great potential for many applications, including all those that involve photonics.

In this talk we will first review different kind of GaAs and InAs nanostructures that can be obtained on an organized fashion on both Si and GaAs substrates. We will include nanostructures in the form of nanowires, nanoneedles and nanoscale membranes [1–3]. Following this, we will elucidate what the photonic properties of these structures are and compare them to what one would observed in standard thin film or bulk form [4]. Finally, we will review how these properties can be used to improve photonic applications such as lasers and solar cells [5,6].

References

- [1] J. Vukajlovic-Plestina *et al*, *Nano Lett.* **17**, 4101 (2017).
- [2] W. Kim *et al*, *Nano Lett.* **18**, 49 (2018)
- [3] G. Tütüncüoğlu *et al*, *Nanoscale* **7**, 19453 (2015).
- [4] Yang *et al*, *Nano Lett.* **17**, 2979 (2017).
- [5] P. Krosgstrup *et al*, *Nature Photon.* **7**, 306 (2013).
- [6] E. Bermudez-Ureña *et al*, *Nano Lett.* **17**, 747 (2017).

Group IV nanowire structure, luminescence and carrier dynamics

P.C. McIntyre

Stanford University, Stanford, California, USA

This presentation will describe the properties of semiconductor nanowires in the Si-Ge-Sn system, in which the nanowire geometry and core-shell structures enable independent control of strain, composition and surface defect passivation. Nanowires of 10 nm to 300 nm diameter are synthesized by locally-catalyzed vapor-liquid-solid crystal growth on both silicon and germanium single crystal substrates. Fundamental photonic and electronic characteristics relevant to nanoscale optoelectronic devices are emphasized.

Highlights include synthesis of single crystal GeSn alloy nanowires with tin content significantly higher than the bulk solubility limit and which exhibit strong direct-gap photoluminescence at room temperature. The nanowire geometry promotes a Sn-stabilized direct gap transition by minimizing compressive misfit strains resulting from 2-dimensional growth on misfitting Ge or Si bulk substrates, providing an exciting approach to group IV semiconductor light emitters. Detailed characterization of strain and compositional variations in Ge-core/GeSn shell nanowires and their effects on luminescence and mid-IR light absorption by the wires will be reported. Carrier dynamics in VLS-grown Ge nanowires are probed by ultrafast pump-probe transient absorption measurements and a systematic modelling methodology. Design rules for use of larger band gap Si, SiGe and germanium oxide shells that suppress non-radiative carrier recombination in Ge-core nanowires are described.

Nitride nanowires on graphene for flexible optoelectronics

*M. Tchernycheva*¹, N. Guan¹, M. Morassi¹, L. Mancini¹, C. Barbier¹, N. Amador¹, A. Kapoor², J. Eymery², C. Durand², L. Lu¹, N. Gogneau¹, A. Madouri¹, F.H. Julien¹, L. Largeau¹, J.-C. Harmand¹

¹ Centre de Nanosciences et de Nanotechnologies, UMR9001 CNRS, University Paris Sud, University Paris Saclay, Palaiseau, France

² University Grenoble Alpes, CEA, INAC, 38000 Grenoble, France

“Photonics Multiannual Strategic Roadmap 2020” mentions flexible electronics, light sources, displays, sensors and solar cells as key emerging technologies with a high expected growth of the market share. Technologies based on organic semiconductors still suffer from a short lifetime and low efficacy as compared to their inorganic counterparts. To make a flexible device from inorganic semiconductors one should shrink the size of the active elements and to integrate them on mechanically-flexible substrates. This can be achieved using control-by-design nanowires.

In this presentation, we address the growth of nitride nanowires on non-conventional substrates and the fabrication and characterization of flexible devices based on nitride nanowires.

First, we will discuss the epitaxy of GaN nanowires on graphene-on-SiO₂ substrates. We show that an excellent selectivity between the graphene and SiO₂ can be achieved. Using this selectivity, organized arrays of nanowires can be synthesized by structuring the graphene layer.

Next, we will discuss the approach for nanowire lift-off, transfer into polymer-embedded membranes and flexible contacting. Realization and characterization of flexible light sources, photodetectors and piezogenerators will be presented.

Advances of quantum dots for lasers and single photon sources

Y. Arakawa

Institute for Nano Quantum Information Electronics, The University of Tokyo

Since the first proposal of the semiconductor quantum dot in 1982 [1], the quantum dots have been intensively investigated for both fundamental solid state physics and device applications. Advances of self-assembling crystal growth technology of quantum dots enabled realization of high performance semiconductor lasers and quantum information devices such as single photon sources. Moreover, implementing a single quantum dot in an optical nanocavity provides a new platform for solid-state cavity quantum electrodynamics (cavity-QED).

In this talk, the current state of the art for the quantum dot lasers and high-performance single photon sources are overviewed. We demonstrate high-performance quantum dot lasers on silicon for optical interconnect technologies [2] and a single photon emission at room temperature from a GaN quantum dot embedded in a nanowire [3,4]. Moreover, recent progress in quantum dot cavity-QED in photonic crystals is discussed, including the observation of a large vacuum Rabi splitting with the record highest value of the figure of merit in the strongly coupled semiconductor quantum-dot-nanocavity systems [5,6] as well as the realization of a topological nanolaser [7].

References

- [1] Y. Arakawa and H. Sakaki, *Appl. Phys. Lett.* **40**, 939 (1982)
- [2] K. Nishi, K. Takemasa, M. Sugawara, *et al* *IEEE J. Sel. Top. Quantum Electron.*, **23** 16921013 (2017).
- [3] M. Holmes, K. Choi, S. Kako, *et al*, *Nano Lett.*, **14** 982 (2014).
- [4] M. Holmes, K. Choi, S. Kako, *et al*, *ACS Photonics* **3** 543 (2016).
- [5] Y. Arakawa, S. Iwamoto, M. Nomura, *et al*, *IEEE J. Sel. Top. Quantum Electron.* **18**, 1818 (2012).
- [6] Y. Ota, D. Takamiya, R. Ohta, *et al*, *Appl. Phys. Lett.* (2018), *in press*
- [7] Y. Ota, R. Katsumi, K. Watanabe, *et al*, *to be submitted for publication*

III-V materials development for nanowire photodetectors and photovoltaics

R.R. LaPierre^{1,2}

¹ Department of Engineering Physics, Centre for Emerging Device Technologies, McMaster University, Hamilton, ON, Canada, L8S 4L7

² ITMO University, Kronverkskiy pr. 49, 197101 St Petersburg, Russia

Abstract. Semiconductor nanowires are being developed for the next generation of optoelectronic devices such as light emitting diodes, lasers, photodetectors, photovoltaics, and transistors. The free lateral surfaces of nanowires allow elastic relaxation of lattice misfit strain without the generation of dislocations, permitting the integration of III-V materials on inexpensive silicon substrates. Furthermore, nanowires permit high optical absorption due to an optical antenna effect. The self-assisted vapor-liquid-solid method is now a well-established technique for the growth of III-V nanowires on silicon substrates. In this method, an array of holes in a SiO₂ film is used for metal droplet collection, which seeds the growth of nanowires. Some of the challenges associated with this technique will be illustrated, using Ga-assisted growth of GaAs nanowires on silicon as an example. A single junction core-shell GaAs nanowire solar cell on Si (111) substrates is presented for photovoltaic and photodetector applications. A Ga-assisted vapor-liquid-solid growth mechanism was used for the formation of a patterned array of radial p-i-n GaAs nanowires encapsulated in AlInP passivation. Novel device fabrication utilizing facet-dependent properties to minimize passivation layer removal for electrical contacting is demonstrated. Electrical characterization and analysis of the cell is reported. The electrostatic potential distribution across a radial p-i-n junction GaAs nanowire is investigated by off-axis electron holography, illustrating the challenges associated with impurity doping for p-n junctions. These characterization methods illustrate some of the challenges in nanowire growth and device fabrication, including dopant incorporation, consumption of the Ga droplet, crystal structure polytypism, surface passivation, and electrical contacting.

Optical and phononic properties of nanowires on demand

M. De Luca

Physics Department, University of Basel, Klingelbergstrasse 82, CH-4056 Basel, Switzerland

III-V semiconductor nanowires (NWs) have been a highly popular area of research during the past decades. The interest in this field is due to the unique properties of the NWs that mostly stem from their large surface to volume ratio, such as the existence of polytypism [1]. Moreover, the ability to mix and match different materials along and around the nanowire in axial and radial heterostructures further enhances their versatility as building blocks of novel electronic and photonic devices.

The polytypism namely the possibility to grow in zincblende (ZB) or wurtzite (WZ) crystal phase, has widened the potential applications of technologically relevant III-V compounds such as GaAs and InP and GaP for which WZ is not available in bulk form and therefore its electronic and optical properties are poorly known. These are key parameters for both optical and electrical applications aimed at implementing novel devices based on WZ NWs or on one-dimensional crystalphase homostructures

Here, the full picture of the WZ band structure of some III-V NWs will be reviewed from both the theoretical and experimental points of view. The electronic band structure was investigated by polarizationdependent photoluminescence (PL) excitation (PLE) spectroscopy. The resulting degree of polarization provides information on the symmetry of the highest valence bands and discloses the subtle yet important role played by excitons on the NW optical dispersion [2,3]. Moreover, by a quantitative analysis of the PL and PLE spectra recorded in the $T = 10-31$ K temperature range we gained insight into the lattice thermal expansion and the extent of the electronphonon interaction [4].

If the capability to control photons and electrons in crystals has brought to an astonishing level of knowledge in fundamental physics as well as to extraordinary technological achievements the manipulation of phonons is still quite unexplored. Such manipulation is a challenging objective, which holds the promise of a step forward in the exploitation of quantum physics and in the manipulation of sound and heat [5] NWs are an ideal platform to explore the novel field of phonon management since they (i) offer the possibility to modify to a large extent the phonon properties by playing with different phonon scattering mechanisms at different length scales; (ii) can be used as a growth template for complex architectures with high degree of freedom on composition/crystal structure/size.

As an example, we consider the case of superlattices in NWs. At variance with conventional 2D superlattices formed by alternating layers with different chemical compositions in NWs it is possible to obtain superlattices by periodically changing only the crystal structure (between WZ and ZB) along the NW axis or by periodically rotating a same crystal structure about the growth axis as in the case of twin superlattices. These approaches ensure atomically sharp interfaces and no interface mixing still providing effective interfaces for phonons owing to the fact that different crystal structures or crystal orientation have different phonon dispersions.

Here we discuss the main properties of the phonon dispersion of ZB and WZ III-V NWs as investigated by microRaman spectroscopy [6]. Moreover, we demonstrate that the existence of a twin superlattice along the crystal growth axis of a NW results in the appearance of new phonon modes besides the longitudinal optical and transverse optical modes existing also in the bulk material with ZB symmetry. We developed a theoretical model able to reproduce the frequency of these new modes at the Γ point of the Brillouin zone taking into account a crystal with a unit cell as long as the superlattice period. We found that the number of modes can be decided *on demand* by tuning the superlattice period thus allowing a controlled design of NW phononic properties.

These results represent the first experimental demonstration of phonon engineering in NWs and are an important step in the investigation of the quantum-mechanical nature of phonons.

References

- [1] P. Caroff *et al.*, *IEEE J. of Selected Topics in Quantum Electronics* **17** 829 (2011).
- [2] M De Luca *et al.*, *Phys. Rev B* **87** 235304 (2013).
- [3] M De Luca *et al.*, *Nano Letters* **15** 998 (2015).
- [4] M De Luca *et al.*, *ACS Nano* **9** 4277 (2015).
- [5] M Maldovan *Nature* **503** (2009). (2013)
- [6] M De Luca, *et al.*, "Semiconductor nanowires: Raman spectroscopy studies" "Raman spectroscopy and applications" Dr Khan Maaz (Ed.), InTech (2017).

Hybrid quantum dot in a nanowire systems

G.E. Cirlin^{1,2,3}, N. Akopian⁴

¹ St Petersburg Academic University RAS, Khlopina 8/3, 194021 St Petersburg, Russia

² ITMO University, Kronverkskiy pr. 49, 197101 St Petersburg, Russia

³ Institute for Analytical Instrumentation RAS, Rizhsky 26, 190103, St Petersburg, Russia

⁴ DTU Photonics, Technical University of Denmark, Kgs. Lyngby, Denmark 2800

A combination of nanowires (NWs) with quantum dots (QDs) are promising building blocks for future optoelectronic devices, in particular, single-photon emitters. The most studied epitaxially grown QDs are self assembled, i.e., grown by island nucleation in the Stranski–Krastanow growth mode. The size, shape, and density of self-assembled QDs can be controlled by changing of the growth parameters such as substrate temperature, growth rate and growth time, but in the end it is a self organized strain induced process and controlling the properties of the array independently is a challenging task. QDs in nanowires have, in contrast, shown great potential as a highly controllable system. The diameter, height, and density of the QDs are defined by the NW diameter, the growth time, and the NW density, respectively, and can be chosen more predictable. Due to a very efficient strain relaxation on the free sidewalls, coherent growth can be much easier realized in the NW geometry, where a small footprint is dictated by a metal catalyst particle assisting the NW growth via the vapor-liquid-solid (VLS) mechanism.

Experimentally, different heteroepitaxial systems were examined. All the samples in the present work were grown by molecular beam epitaxy (MBE). For AlGaAs/GaAs material systems, different growth conditions were applied, but the strategy was the same: we have used Au-assisted growth of the NWs on Si(111) substrate, firstly we grew the AlGaAs base of the NW, secondarily, the GaAs nanoinsertion with lower bandgap (typically during 5–25 s), or QD, was formed and we end the structure with the core with the same material as the base. It was found that during the growth spontaneous, independently on the Al fraction, core-shell structures with lower aluminum content in the cores are formed. Another important conclusion is that aluminum should enter the droplet at a much lower rate but leave the droplet at a much higher rate than gallium. Optically, our growth method results in the formation of GaAs QD in a AlGaAs NW having very narrow spectral linewidth ($< 10 \mu\text{eV}$), single-photon emission in the wavelength range 75–82 nm in dependence on the QD growth time.

Another example in AlGaAs system is crystal phase quantum dots. In semiconducting nanowires, both zinc blende and wurtzite crystal structures can coexist. The band structure difference between the two structures can lead to charge confinement. Electrons (and holes) can be confined in two other dimensions, perpendicular to the growth direction. The three-dimensional confinement will form a crystal phase quantum dot — it is formed from two different crystalline phases of the same material. Their radiative recombination with holes in adjacent wurtzite parts of a NW may therefore be a source of single photons. The zinc blende segments lengths set the confined electrons energy levels. The indirect radiative recombination will again result in longer lifetimes due to reduced overlap of electron and hole wave functions. Hence, a crystal phase QD is formed for both electrons and holes

Additionally, we report on the synthesis of InAsP insertions in InP nanowires grown on Si(111) substrates by Au-assisted MBE. We show that the the total amount of Au deposited growth and relatively low substrate temperature allows us to control the nucleation on the NW lateral surface and provide a method to embed InAsP insertions into InP shells. For InP/InAsP/InP heterostructure formation, the growth started with 15 min of InP, then the As source was opened for 2–30 s in order to form an InAsP segment in each NW. In some cases, the As to P flux ratio was varied from sample to sample to investigate different alloy compositions. The growth was completed with 5 min deposition of InP. When a shell is present, the resulting heterostructures demonstrate strong room-temperature photoluminescence with a peak wavelength tunable from 1.3 to 1.45 μm by adjusting the growth conditions.

Self-assembled formation of GaN nanowires on amorphous substrates

Z.R. Zytewicz

Institute of Physics, Polish Academy of Sciences, Al. Lotnikow 32/46, 02-668 Warszawa, Poland

It is well established that GaN nanowires (NWs) are promising building-blocks of new electronic and optoelectronic devices. Much effort is recently concentrated on controlled growth of GaN NWs on non-crystalline substrates, which offers a large degree of freedom in designing new devices. Actually, formation of GaN NWs on SiO₂ [1–4] and Al_xO_y [5–7] buffers, silica or quartz substrates [8–10], TiN [11] and Mo [12] films, as well as on Ti [13,14] and Ta [14] metallic foils has been reported already. However, due to the lack of fundamental growth studies, the growth mechanisms underlying the formation of GaN NWs on non-crystalline substrates are still not well understood, hindering the control of the growth process.

In this talk we will present a comprehensive description of the self-assembled nucleation and growth of GaN NWs by plasma-assisted MBE (PAMBE) on amorphous Al_xO_y (a-rm Al_xO_y) buffers prepared at low temperature by atomic layer deposition. Reflection high-energy electron diffraction (RHEED) and line-of-sight quadrupole mass spectrometry (QMS) have been used for *in-situ* monitoring of microscopic processes of nucleation and growth of GaN NWs. They are compared with analogous processes occurring under otherwise identical growth conditions on nitridated Si — the substrate commonly used for MBE growth of GaN NWs. In this way, a general understanding of the formation of GaN NWs is sought, with particular emphasis on the role of the substrate and its influence on the growth process.

Qualitatively, we have observed the same nucleation and growth phenomena on both substrates. The formation and growth of NWs proceed in three different stages: initially, during an extended incubation time no GaN forms, as we have confirmed by SEM and AFM studies of dedicated samples with different growth durations. Then, the formation of GaN nuclei is indicated by the appearance of the corresponding reflections in RHEED, and as their number continuously increases the incorporated Ga flux determined by QMS rises steeply. During this stage, the shape of the GaN islands changes from spherical cap to the NW morphology, as was reported before for nitridated Si substrates [15]. Finally, further anisotropic growth of NWs takes place and collective effects lead to an equilibration of the NW heights in the ensemble, again similarly to growth on nitridated Si [16,17]. All the similarities found for experiments on a-Al_xO_y and nitridated Si imply that the nucleation and growth mechanisms elucidated by numerous in-depth studies for the self-assembled formation of GaN NWs by PAMBE on the latter type of substrate are not limited to that particular substrate but are general in nature. Consequently, this type of NW formation is inherent to GaN growth by PAMBE and should be transferable to numerous types of substrates.

Quantitatively, however, there are differences in the GaN nucleation on the two types of substrates studied here. More specifically, the QMS and RHEED observations have revealed

that on a-Al_xO_y the incubation time is much shorter than on nitridated Si under the same conditions of Ga and N fluxes and the growth temperature. Dependence of RHEED measured incubation time on Ga flux and temperature has been modelled indicating that enhanced GaN nucleation is due to heterogeneous nucleation mechanism on amorphous Al_xO_y while the less efficient, homogeneous nucleation dominates on nitridated Si [18]. Moreover, the critical dimensions at which the shape transition takes place are different. In particular, the critical height of GaN nuclei on a-Al_xO_y is more than six times larger than for those on nitridated Si, while their critical radius is only slightly larger.

Finally we will show that under proper growth conditions, GaN NWs with excellent structural and optical properties, as observed by SEM, TEM, XRD and PL techniques, can be formed by PAMBE on a-Al_xO_y buffers. In this way, our results pave the way to the crystallization of high quality GaN NWs on any substrate, provided it is compatible with the MBE technology and its surface is covered by a thin a-Al_xO_y buffer layer.

Acknowledgements

This work was partially supported by the Polish National Science Centre Grants No. 2016/21/N/ST3/03381, 2016/23/B/ST7/03 and 2016/21/B/ST5/03378.

References

- [1] T.T. Stoica, *et al.*, *Small* **4**, 751 (2008).
- [2] S. Zhao, *et al.*, *Nanoscale* **5**, 5283 (2013).
- [3] Y. Park, *et al.*, *Opt. Exp.* **23**, A650 (2015).
- [4] A. Liudi Mulyo *et al.*, *J. Crystal Growth* **480**, 67 (2017).
- [5] M. Sobanska *et al.*, *J. Appl. Phys.*, **115**, 043517 (2014).
- [6] M. Sobanska *et al.*, *J. Appl. Phys.*, **118**, 184303 (2015).
- [7] M. Sobanska *et al.*, *Nanotechnology*, **27**, 325601 (2016).
- [8] Y. Zhao, *et al.*, *J. Semicond.* **35**, 093002 (2014).
- [9] S.-Y. Bae, *et al.*, *Sci. Rep.* **7**, 45345 (2017).
- [10] V. Kumaresan, *et al.*, *Nanotechnology* **27**, 135602 (2016).
- [11] W. Wolz, *et al.*, *Nano Lett.* **15**, 3743 (2015).
- [12] ATM G. Sarwar, *et al.*, *Small*. **11**, 5402 (2015).
- [13] G. Calabrese, *et al.*, *Appl. Phys. Lett.* **108**, 202101 (2016).
- [14] B.J. May, *et al.*, *Appl. Phys. Lett.* **108**, 141103 (2016).
- [15] V. Consonni, *et al.*, *Phys. Rev. B* **83**, 035310 (2011).
- [16] S. Fernandez-Garrido, *et al.*, *Nano Lett.* **15**, 1930 (2015).
- [17] K.K. Sabelfeld, *et al.*, *Appl. Phys. Lett.* **103**, 133105 (2013).
- [18] M. Sobanska, *et al.*, *Cryst. Growth Des.* **16**, 7205 (2016).

“Stopping” effect and its role in oscillations of truncation in III-V nanowires

V.G. Dubrovskii^{1,2}, F. Glas³, G. Patriarche³, F. Panciera³, J.-C. Harmand³

¹ ITMO University, Kronverkskiy pr. 49, 197101 St Petersburg, Russia

² Ioffe Institute, Politekhnicheskaya 26, 194021 St Petersburg, Russia

³ Centre for Nanoscience and Nanotechnology, CNRS, Université Paris-Sud, Université Paris-Saclay, Route de Nozay, Marcoussis 91460, France

In-situ studies of the VLS growth of vapor-liquid-solid (VLS) nanowires reveal truncated growth interfaces which oscillate in synchronization with the nucleation pulses [1,2]. The presence or absence of truncation depends on the contact angle of the droplet and is often thought to determine the crystal structure of III-V NWs (zincblende in truncated NWs at larger contact angles and wurtzite in planar NWs at smaller contact angles) [2]. Here, we will consider how the stopping effect [3] influences the truncated volume in Au-catalyzed GaAs NWs studied by *in-situ* NanoMax TEM [4].

We model the interface oscillations using the normalized free energy difference of forming the interface with and without truncation [4]

$$g(x) = -4px^{1/2} + 2\varphi x + x^2.$$

Here, $x = k/i_{\max}$ is the relative truncated volume in the units of the monolayer (ML) volume i_{\max} , and p is the surface energy contribution which is positive when the truncated facet is preferred on surface energetic grounds [2], and This potential also depends on

$$\varphi = [i_s - (i - l)]/i_{\max}.$$

Here, i is the number of III-V pairs in the growing 2D island, l is the number of III-V pairs brought into the droplet from vapor and i_s is the “stopping” size at which the island cannot grow any more without refill from vapor. Clearly, $(i - l)/i_{\max}$ oscillates from zero to unity and back to zero in each monolayer (ML) growth cycle, which is why φ changes its sign from positive to negative and back at $i = i_s$ when $i_s < i_{\max}$.

Using this, we show that the amount of truncation can start from zero and return to zero in each ML growth cycle [4]. Hence 2D islands can nucleate at the trijunction in the planar geometry of the liquid-solid interface, which supports the earlier models of polytypism in III-V NWs [5,6]. The necessary condition for such oscillations is the existence of the stationary size above which the island cannot grow from liquid any more. If kinetics permits, 2D islands are further fed by developing the truncated edge. This process is faster than refill from vapor. We can see oscillating truncated facets in Au-catalyzed GaAs NWs grown at higher III/V flux ratios, corresponding to larger contact angles of the droplets. For a given NW radius, the stationary size may decrease simply because the gallium-rich conditions at high III/V ratios decrease the arsenic content in the droplet. The amount of truncation described by our model can be much larger than in the earlier model of Tersoff [2], particularly in the case of high chemical potentials typically employed under the real MBE growth conditions.

Acknowledgements

The financial support of the Russian Foundation for Basic Research under grants 17-52-16017, 16-29-03129, and 16-02-00134 is gratefully acknowledged.

References

- [1] D. Jacobsson *et al.*, *Nature* **531**, 317 (2016).
- [2] C.-Y. Wen *et al.*, *Phys. Rev. Lett.* **107**, 025503 (2011).
- [3] V. G. Dubrovskii, *Cryst. Growth Des.* **17**, 2544 (2017).
- [4] J. C. Harmand *et al.*, to be published (2018).
- [5] F. Glas, J. C. Harmand, G. Patriarche, *Phys. Rev. Lett.* **99**, 146101 (2007).
- [6] V. G. Dubrovskii *et al.*, *Phys. Rev. B* **78**, 235301 (2008).

Small angle X-ray scattering of a stretchable photonic crystal

A.M. Korsunsky^{1,2}, I.P. Dolbnya³, T. Sui⁴, J.J. Baumberg⁵, Q. Zhao⁵

¹ MBLEM, Department of Engineering Science, University of Oxford, Parks Rd, Oxford OX1 3PJ, UK

² Skolkovo Institute of Science and Technology, 3 Nobel st., Moscow 143026, Russia

³ Diamond Light Source, Harwell, Oxford Didcot OX11 0DE, UK

⁴ Department of Mechanical Engineering Sciences, University of Surrey, Guildford, UK

⁵ Nanophotonics Centre, Cavendish Laboratory, Department of Physics, Univ. of Cambridge, Cambridge CB3 0HE, UK

Colloidal crystals are formed by ordered arrangement of micro-to nanoparticles that may arise in solution or during sedimentation under the action of interactive forces and the influence of steric effects that lead to packing that is reminiscent of that found in crystals. Colloidal crystals drew attention and became the subject of extensive study due to the wide range of interesting phenomena they display, e.g. the influence of particle shape, electrostatic forces, surface tension and gravity etc. on the arrangements that arise. The lattice period of colloidal crystals that emerge may lie in the range that allows strong interaction and scattering of UV, visible and IR light. Another cause of sustained interest is that colloidal crystals may be thought of as models of real atomic or molecular crystals that are scaled up several orders of magnitude.

Recently, it was proposed to create photonic crystals known as polymer opals through consolidating core-shell polymer particles with harder polymer at the centre (e.g. polystyrene, PS, or poly(methyl methacrylate), PMMA) and elastomeric outer layer (e.g. poly(ethyl acrylate), PEA) and subjecting them to repeated reverse shear to induce ordering into a regular arrangement [1]. A key advantage of such polymer opals lies in the fact that they can potentially be produced on a vast scale, and that their large capacity for elastic (or nearly elastic) deformation allows their photonic properties to be changed and tuned simply by stretching.

In this context, it is of clear interest to study the behaviour of the elastomer matrix with hard spherical nanoparticles embedded in it. Of the many different approaches available, the use of small angle X-ray scattering (SAXS) is of particular interest, as it is a non-destructive and non-disturbing technique that allows observing structural changes in reciprocal space whilst the specimen undergoes deformation. An interesting aspect of SAXS from colloidal crystals and opals is that the scattering patterns obtained are similar in their appearance and interpretation to those typically seen in the wide angle X-ray scattering (WAXS) regime from regular crystals.

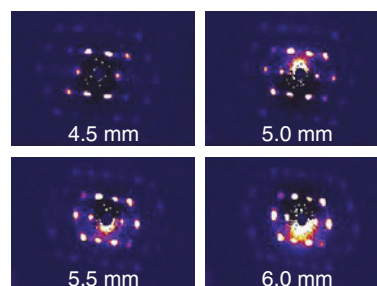


Fig. 1. Illustration of the evolution of small angle X-ray scattering (SAXS) patterns during *in situ* stretching of a polymer opal (labels below indicate extension in mm).

Figure 1 illustrates a sequence of diffraction patterns obtained during *in situ* stretching of a polymer opal film. Details of the experimental setup and interpretation of the patterns in terms of ‘lattice’ deformation and distortion will be presented and discussed.

References

- [1] Q.B. Zhao, *et al.*, *Nat. Comms.* **7** 11661 (2016).

Guided nanowire optoelectronics

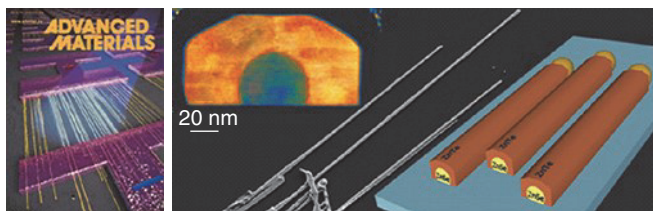
E. Joselevich

Department of Materials and Interfaces, Weizmann Institute of Science, Rehovot 76100, Israel

The large-scale assembly of NWs with controlled orientation on surfaces remains one challenge toward their integration into practical devices. During the last few years we reported the growth of perfectly aligned, millimeter-long, horizontal NWs of GaN [1], ZnO [2], ZnSe [3], ZnTe [4], CdSe [5], CdS [6], CsPbBr₃ [7] and other materials, with controlled crystallographic orientations on different planes of sapphire [1–7], SiC [8], quartz [9], and spinel [10]. The growth directions and crystallographic orientation of the NWs are controlled by their epitaxial relationship with the substrate, as well as by a graphoepitaxial effect that guides their growth along surface steps and grooves. As a proof of concept for future applications, we demonstrated the massively parallel “self-integration” of NWs into circuits via guided growth [11]. Here we will show how guided nanowires with complex morphologies and heterostructures can be used for the bottom-up fabrication of nano-optoelectronic devices, including photodetectors, photodiodes and photovoltaic cells [12].

References

- [1] *Science* **2011** 333, 1003
- [2] *ACS Nano* **2012** 6, 6433
- [3] *Adv. Mater.* **2015** 27, 3999
- [4] *J. Phys. Chem. C*, **2016** 120, 18087
- [5] *ACS Nano* **2017** 11, 213
- [6] *J. Am. Chem. Soc.* **2017** 139, 15958
- [7] *Nano Lett.* **2018** 18, 424
- [8] *Nano Lett.* **2013** 13, 5491
- [9] *ACS Nano* **2014** 8, 2838
- [10] *J. Phys. Chem. C* **2014** 118, 19158
- [11] *Proc. Nat. Acad. Sci. USA* **2013** 110, 15171
- [12] *ACS Nano* **2017** 11, 6155



Self-catalyzed molecular beam epitaxy of GaAs nanowires for photonic applications

T. Hakkarainen¹, E. Koivusalo¹, M.R. Piton^{1,2}, E. Petronijevic³, G. Leahu³, A. Belardini³, M. Centini³, C. Sibilia³, V.G. Dubrovskii^{4,5}, M. Guina¹

¹ Optoelectronics Research Centre, Tampere University of Technology, Tampere Finland

² Departamento de Física, Universidade Federal de São Carlos, São Carlos (SP), Brazil

³ SBAI Department, Sapienza University of Rome, Rome, Italy

⁴ ITMO University, St Petersburg, Russia

⁵ Ioffe Institute, St Petersburg, Russia

III-V semiconductor nanowires (NWs) are widely considered as one of the most promising building blocks for nanoscience and nanotechnology. Size uniformity within the NW ensembles in terms of both diameter and length is important for applications and interesting from a fundamental point of view. A single semiconductor NW has good waveguiding properties and can support a number of photonic modes in the visible — near-IR part of the spectrum. These size-dependent light confining properties are essential for several NW-based application including lasers, solar cells, and photodetectors, which set a demand for precise control over the NW dimensions.

Here, we discuss recent progress in self-catalyzed growth of uniform GaAs NWs on Si(111) wafers pre-patterned using a lithography-free technique. Namely, the method is based on droplet epitaxy and spontaneous oxidation, which allows con-

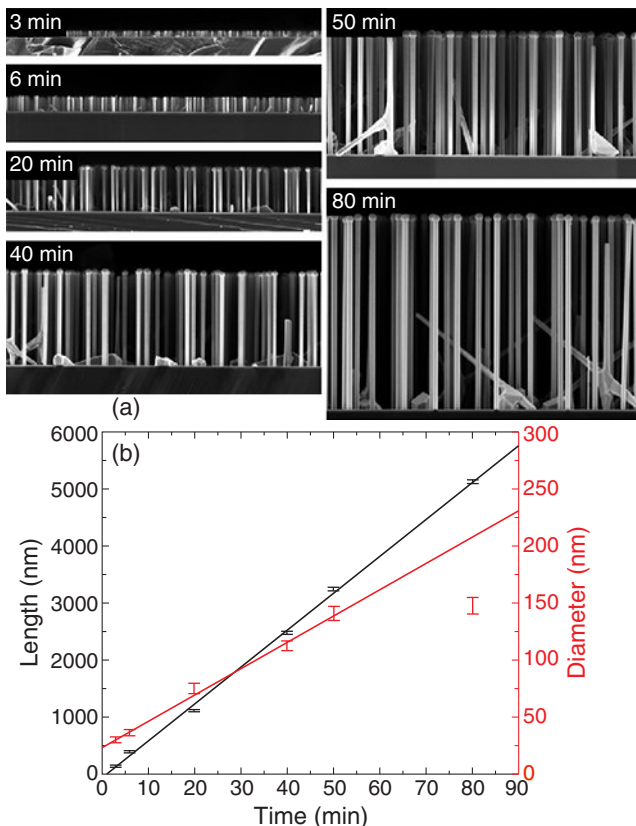


Fig. 1. (a) The evolution of GaAs NW length during self-catalyzed growth. The scale bar is 1 μm . (b) Mean values of the NW length and diameter presented with their standard deviations.

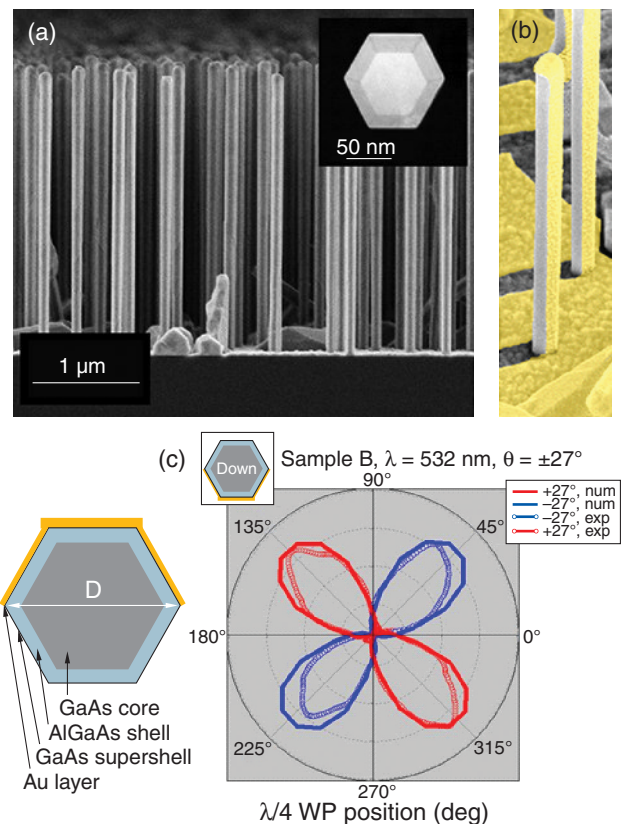


Fig. 2. (a) SEM picture of GaAs-AlGaAs-GaAs core-shell NWs. (b) False colour SEM picture of asymmetrically Au-coated core-shell NWs. (c) Circular dichroism measured by photo-acoustic technique for the Au-coated NWs. The incident angle is either -27° or 27° with respect to the NW axis. The Au-coated side of the NW is located in the plane of incidence.

trolling the size and density of the NW nucleation sites [1,2]. We have recently shown that the NWs grown on such templates retain remarkable size uniformity throughout the growth (as seen in Fig. 1) and results in the first demonstration of sub-Poissonian length distribution [3].

The photonic properties of the uniform NWs are then investigated using photo-acoustic technique, which is a versatile scattering-free method for revealing the photonic modes in as-grown NW ensembles [4]. The control of the resonant wavelength is demonstrated by AlGaAs shell growth. Furthermore, a new type of semiconductor-metal hybrid structure was formed by asymmetrically Au-coating the core-shell NWs, as

shown in Fig. 2. Although not inherently chiral, the Au-coated NWs exhibit extrinsic when the experimental configuration is chosen properly. This requires (i) tilting of sample away of normal incidence and (ii) such azimuthal angle that the Au-coated side of the NW is located in the plane of incidence (up or down when the beam is coming from right or left). These conditions give rise to extrinsic chirality due to breaking of symmetry. In such conditions the Au-coated NWs exhibit chiral optical response in both absorption [5] and emission. Furthermore, superchiral fields can be excited in these structures using linearly polarized light [6] which can be further exploited in chiral sensing applications.

References

- [1] T.V. Hakkarainen *et al.* *Nanotechnology* **26**, 275301 (2015).
- [2] E.S. Koivusalo *et al.* *Nanoscale Research Letters* **12**, 192 (2017).
- [3] E.S. Koivusalo *et al.* *Nano Letters* **17**, 5350, (2017).
- [4] G. Leahu *et al.* *Scientific Reports* **7**, 2833 (2017).
- [5] G. Leahu *et al.* *Advanced Optical Materials* **5**, 1601063 (2017).
- [6] E. Petronijevic *et al.* *Optics Express* **25**, 14148 (2017).

New opportunities at European XFEL

R. Feidenhans'l

European XFEL, Holzkoppel 4, 22869 Schenefeld, Germany

The European X-ray Free Electron Laser is the brightest X-ray free electron laser in the world. Due to its superconducting accelerator it will be able to deliver up to 27000 intense, ultrashort X-ray pulses per second. The facility started commissioning in 2017 and went into operation July 1 2017. First lasing at hard x-ray energies was observed in May 2017 on the first set of instruments. Lasing was achieved in February 2018 on the second set of instruments.

User experiments have been conducted since September last year. The first two instruments that opened for user experiments were the FXE instrument for ultra-fast x-ray spectroscopy and x-ray scattering and the SPB/SFX instrument for diffractive imaging and structural determination for single particles, clusters and biomolecules. This year two more

instruments will be taken into operation and the last two instruments will go on-line in 2019. In total this will cover a wide range of scientific fields from biology to material science opening up new areas of science in particular within ultrafast dynamics.

In the talk I will give a description of the facility [1] including a status report of the operation, a glimpse into results from the first experiments and an outlook into the prospects for the coming years.

References

- [1] T. Tschentscher, C. Bressler, J. Grunert, *et al* *Appl. Sci.*, **7**, 592 (2017); doi:10.3390/app7060592.

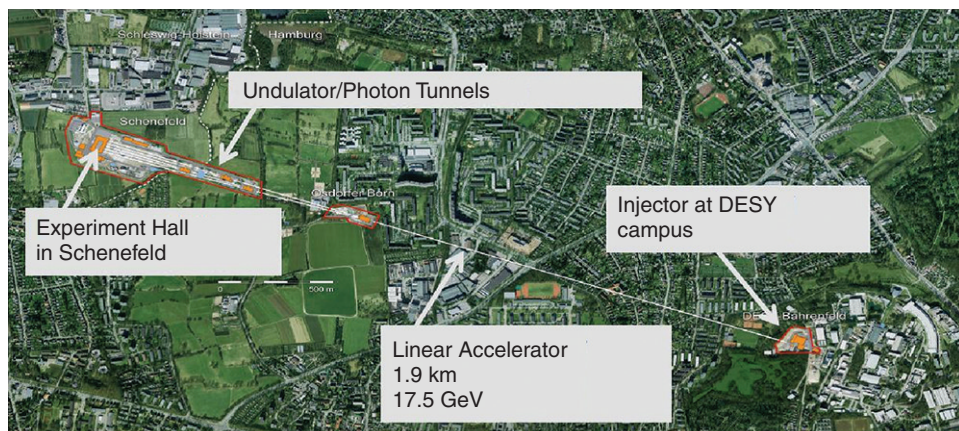


Fig. 1. Outline of European XFEL.

Low temperature plasma deposition processes: from amorphous silicon to epitaxial growth and nanowires

P. Roca i Cabarrocas

LPICM, CNRS, Ecole Polytechnique, Universite Paris-Saclay, 91128 Palaiseau Cedex, France

Silicon thin film technology has been driven by hydrogenated amorphous and microcrystalline silicon thin films which are routinely produced using silane plasmas. While SiH_3 is often considered as the main radical for the obtaining of such films, we have shown that changing the process to conditions where silicon clusters and nanocrystals are produced in the plasma can lead to high deposition rates and improved materials, such as hydrogenated polymorphous silicon and polycrystalline silicon [1]., by changing the substrate from glass to crystalline silicon, it is possible to produce epitaxial crystalline silicon films (c-Si:H) which can be transferred to foreign substrates [2,3]. Interestingly enough the structure of c-Si:H films is found to be tetragonal, indicative of their particular growth process [4]. Even more interesting, this low temperature epitaxial process can be extended to doped films as well as to germanium and silicon-germanium alloys and their heteroepitaxial growth on GaAs [5]. Last but not least, combining PECVD with low melting temperature metal nanoparticles such as indium and tin opens the way to the growth of nanowires (including Ge, Si and GeSn), which allow to achieve efficient light trapping and carrier collection in radial junction solar cells [6] or even to growth the c-Si nanowires in-plane for stretchable electronics and photonics applications [7].

References

- [1] Ka-Hyun Kim *et al. Sci. Reports* **7** 40553 (2017)
- [2] R. Cariou *et al. Prog. in Phot.: Research and Applications* **24** 1075-1084 (2016)
- [3] A. Gaucher *et al. Nano Letters* **16** 5358 (2016)
- [4] W. Chen, *et al. Crystal Growth and Design* **17** 4265 (2017)
- [5] G. Hamon, *et al. J. Photon. Energy* **7** (2), 022504 (2017)
- [6] S. Misra *et al. J. Phys. D: Appl. Phys.* **47** 393001 (2014)
- [7] Zhaoguo Xue *et al. Nature Communications* **7** 12836 (2016)

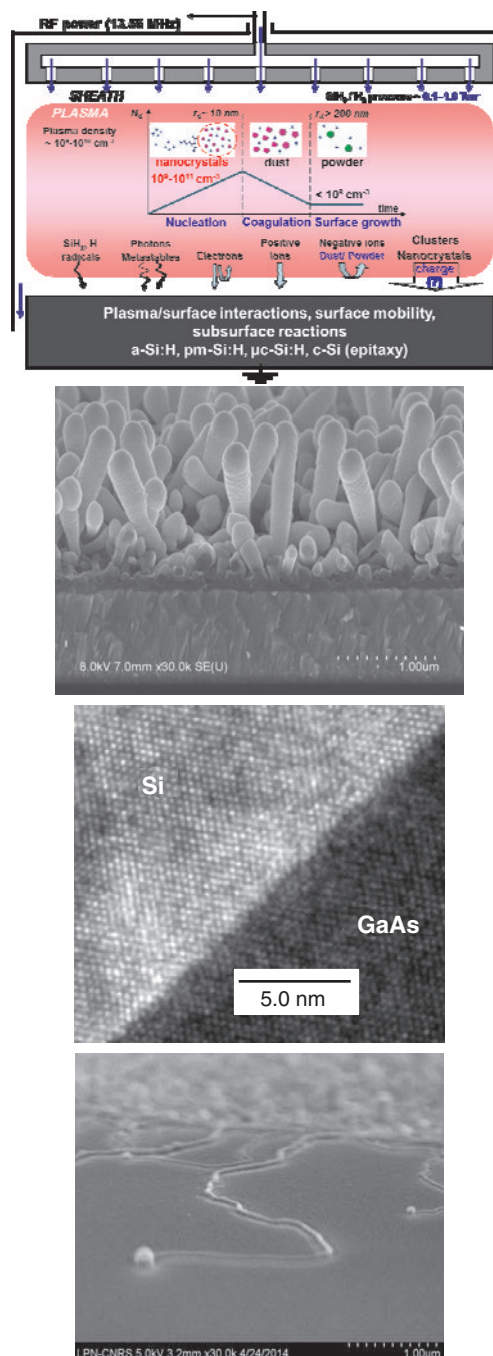


Fig. 1. Schematic diagram of a RF glow discharge reactor. A wide range of thin films can be obtained, from a-Si:H to ordered epitaxial films and silicon nanowires

Intervalley mixing due to interfaces in semiconductor nanostructures

M.O. Nestoklon

Ioffe Institute, 194021, Politekhnikeskaya 26, Saint Petersburg, Russia

In the nanostructures based on multivalley semiconductors, the valley index is not a good quantum number: at the heterointerfaces the translational invariance is lifted and the states from different valleys mix. Intervalley mixing and its effect on electron states and optical properties are discussed in nanocrystals (NCs) [1] and nanowires (NWs) [2] of Pb chalcogenides, Si/SiGe quantum wells (QWs) [3], Ge/Si quantum dots (QDs) [4] and (In,Ga)As/GaP QDs [5].

The valley splitting is studied in PbSe and PbS NCs [1] and NWs [2]. In these materials, the extrema of the conduction and valence bands are located at four inequivalent L points of Brillouin zone. To describe the properties of the nanostructures, one has to take into account the valley mixing due to quantum confinement and the anisotropy of the effective masses. In the tight-binding method, spherical NCs and cylindrical NWs are considered, but with the different position of their centres with respect to crystall lattice sites. Microscopic calculations show that the symmetry affects the valley and spin splitting of the quantum confined states. E.g., in NCs without inversion centre the valley and the spin splitting is significantly suppressed. This phenomenon is unusual: in general, higher symmetry leads to higher degeneracy of the levels, while in this case the situation is opposite.

Also, the valley and spin splitting in Si/SiGe QWs are considered. In such quantum wells grown along [001] direction, in the effective Hamiltonian of electrons symmetry allows two linear-in-k terms. The constants which define the magnitude of these terms depend on the oscillations of the valley splitting as a function of QW width [3]. This phenomenon is studied in the combination of atomistic tight-binding calculations and the generalized envelope function approach. Analytical approach with five parameters perfectly reproduces the results of complex atomistic approach.

Then the reconstruction of the spectrum in the core-shell Ge/Si QDs is discussed. It is shown that the Si shell of the monolayer thickness is enough to reduce the radiative recombination rate due to L-X crossover [4]. The shell also leads to strong redshift of the photoluminescence (PL). Electron spectrum and the rates of the radiative transitions are calculated in the advanced tight-binding method. To analyse the valley structure of the states obtained in atomistic approach, we use the analysis of the local density of states in reciprocal space. This approach allows to show (1) that the transition to the type-II heterostructure in real and reciprocal spaces take place at different shell thickness and (2) the valley crossover is more important for the decrease of optical transitions rate than the spacial localization of the electrons.

The optical properties of the (In,Ga)As/GaP QDs are also discussed. In the atomistic tight-binding their electronic and optical properties are calculated, it is shown that the transitions between the holes localized inside the QDs and the electrons from X_Z valleys in GaP matrix localized by the strain field play the main role in the optical properties of this system [5]. The strain field is calculated for the large supercell in the valence force field method and the electron states are calculated in $sp^3d^5s^*$ tight-binding method. For the ground electron state, the wave function of the electron is not localized inside the QD, but in the matrix close to QD apex. The Fourier transform of the ground state shows that it is the X_Z valley state (more than 95%) with a small admixture of Γ point. The redshift of the photoluminescence spectrum under hydrostatic pressure is in a good agreement with the value of the deformation potential for X-valley electrons.

References

- [1] A.N. Poddubny, M.O. Nestoklon, S.V. Goupalov, *Phys. Rev. B* **86**, 035324 (2012).
- [2] I.D. Avdeev, A.N. Poddubny, S.V. Goupalov, and M. O. Nestoklon, *Phys. Rev. B* **96**, 085310 (2017).
- [3] M.O. Nestoklon, L.E. Golub, E.L. Ivchenko, *Phys. Rev. B* **73**, 235334 (2006).
- [4] M. O. Nestoklon, A. N. Poddubny, P. Voisin, K. Dohnalova, *Jour. Phys. Chem. C* **120**, 18901 (2016).
- [5] C. Robert, K. Pereira Da Silva, M.O. Nestoklon, *et al*, *Phys. Rev. B* **94**, 075445 (2016).

Flexible optoelectronic devices based on III-nitride nanowires

N. Amador¹, N. Guan¹, X. Dai¹, H. Zhang¹, V. Piazza¹, A. Kapoor^{2,3}, C. Bougerol^{2,4}, L. Mancini¹, F. H. Julien¹, H. Chalermchai¹, A. Cattoni¹, S. Collin¹, F. Oehler¹, J.-C. Harmand¹, J. Eymery^{2,3}, C. Durand^{2,3} and M. Tchernycheva¹

¹ C2N site Orsay and Marcoussis, UMR 9001 CNRS, Univ. Paris Sud, Univ. Paris Saclay, 91405 Orsay, France

² Université Grenoble Alpes, 38000 Grenoble, France

³ CEA-CNRS “Nanophysique et Semiconducteurs” group, CEA-INAC-PHELIQS, 17 rue des Martyrs, Grenoble 38000, France

⁴ CEA-CNRS “Nanophysique et Semiconducteurs” group, CNRS, Institut Neel, 25 rue des Martyrs, 38000 Grenoble, France

Flexible electronics, flexible light sources, displays and solar cells are key emerging technologies. Indeed, flexible devices offer new functionalities inaccessible with conventional technologies (e.g., rollable screens, bendable or implantable light sources, energy harvesters integrated in clothing, etc.). Technologies based on organic semiconductors still dominate the market, however organic devices suffer from a short lifetime and low efficiency. Inorganic devices offer a long lifetime and high efficiency but they are usually fabricated in form of thin films presenting a rigid structure.

Semiconductor nanowires accommodate the lattice mismatch with the substrate resulting in single crystals fully relaxed and free of dislocations. The high material quality of the nanowires improves their optical and electrical properties, making these structures very promising candidates for a new generation of high efficiency devices. In addition, they are characterized by a small footprint, high mechanical flexibility and long-term stability, making them excellent candidates for flexible devices. Optoelectronic devices based on nanowires can potentially reach high efficiencies both for light emission and for detection and at the same time enable mechanical flexibility.

Group III-nitride materials offer excellent properties for light emission applications due to their direct bandgap, that can be tuned over a very wide range of wavelengths, from 1900 nm for the InN in the infrared, to 360 nm for GaN until 210 nm for the AlN in the C-Ultraviolet.

In our work, we make use of nitride nanowires as an active material for flexible LEDs. Polymer-embedded nanowires offer an elegant solution to create flexible optoelectronic devices, which combine the high efficiency and long lifetime of inorganics semiconductor materials with the high flexibility and transparency of polymers.

We used self-assembled GaN nanowires grown on c-sapphire substrate by catalyst-free metalorganic chemical vapor deposition (MOCVD) [1]. These nanowires (length $\sim 20 \mu\text{m}$, radius $\sim 1.0 \mu\text{m}$) have a core/shell n-p junction incorporating radial InGaN/GaN multiple quantum wells. The emission color is controlled by changing the In concentration of the InGaN quantum wells. The nanowires were encapsulated into a PDMS membrane and mechanically peeled-off their growth substrate. Then the membrane was contacted using spin-coated silver nanowires, which form a transparent and mechanically flexible contact.

Following these procedures, blue and green flexible nanowire LEDs were fabricated [2]. Moreover, white flexible LED was fabricated, by blue light down conversion with yellow

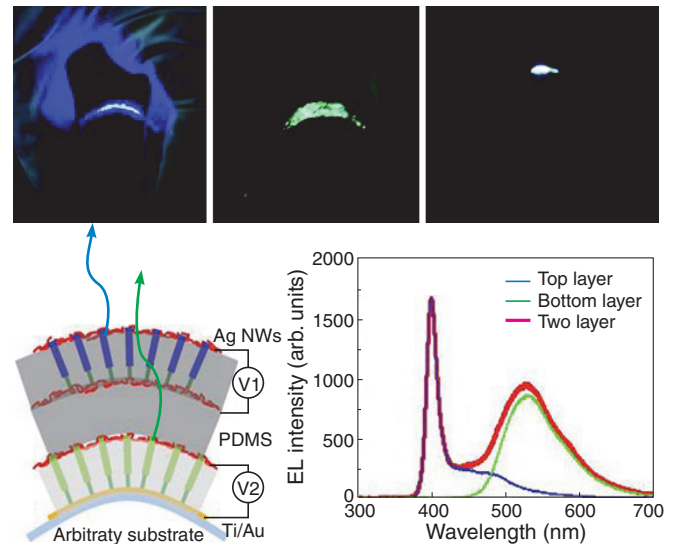


Fig. 1. Top: flexible nanowire blue, green and white LEDs under operation. Bottom: schematic and electroluminescence spectra of a two-color LED.

nano-phosphors, achieving white light by blue yellow mixture [3]. Pictures of these three different devices are shown in Fig. 1.

Our approach offers the possibility to assemble free-standing layers of nanowire materials with different bandgaps without any constraint related to lattice-matching or growth conditions compatibility. This concept therefore provides a large design freedom and modularity since it enables combination of materials with very different physical and chemical properties, which cannot be achieved by monolithic growth. Making use of this modularity, a two-color device was fabricated. Combining two flexible LED layers containing different active material nanowires as illustrated in Fig. 1.

We are presently working on the realization of the third red layer emitting red light. GaAsP nanowire grown by MBE on prepatterned substrates are explored for the red emission. The objective is to achieve a white flexible LED by combining red, green and blue light and thus eliminate the down-conversion losses.

Because of the smaller size of MBE-grown nanowires, the fabrication procedures (namely, the polymer encapsulation and peel off steps) should be revisited.

As a perspective, development of pixels to move towards flexible displays is underway.

References

- [1] R. Koester, J. Hwang, D. Salomon, *et al*, *Nano letters*, **11**, 4839–4845 (2011).
- [2] X. Dai, A. Messanvi, H.i Zhang, *et al*, *Nano Letters* **15**, 6958–6964 (2015).
- [3] N. Guan, X. Dai, A. Messanvi *et al*, *ACS Photonics* **3**, 597–603, (2016).

Cadmium telluride nanowire growth for photovoltaic application

Manuel Apollo¹, Jon Major¹, Wojciech Stepniowski^{2,3}, Massimo Tormen⁴ and Ken Durose¹

¹ Stephenson Institute for Renewable Energy/Dept of Physics, University of Liverpool, L69 7ZD, UK

² Lehigh University, Department of Materials Science & Engineering 5 East Packer Ave. 18015 Bethlehem, PA, USA

³ Department of Advanced Materials and Technologies Military University of Technology Urbanowicza 2 Str. 00908 Warszawa, Poland

⁴ ThunderNIL Srl, Area Science Park, Basovizza, I-34149, Trieste, Italy

There is a global drive to increasing the efficiency, performance and cost effectiveness of renewable energy sources including the photovoltaic (PV) devices. Currently the PV market is dominated by silicon (Si) solar cells technology. Although their performances, they suffer technological limitations, such as an indirect bandgap and low absorption coefficient.

An alternative material like cadmium telluride (CdTe), a II-VI semiconductor, exhibits a direct bandgap of approximately 1.45 eV, which enables optimal absorption of the solar radiation. Therefore high efficiency CdTe solar cells are thinner and more economically convenient than Si solar cells [1]. In Figure 1 typical CdTe solar cells are shown.

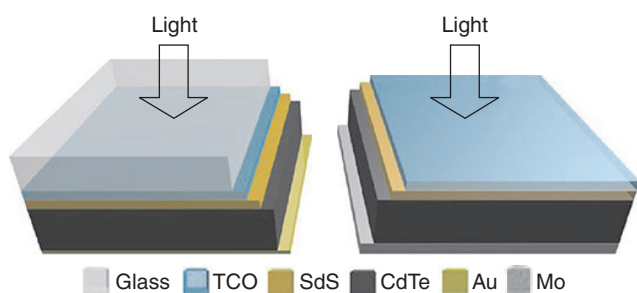


Fig. 1. Schematic diagram of typical CdTe solar cells adopting the “superstrate” (left) and “substrate” (right) configuration.

In addition, it is possible that nanostructures may be used to create new kinds of devices with enhanced optical performance over existing structures. It is the aim of our project to explore these opportunities, in particular the possibility of growing nanowires (NWs) in the template assisted method, using aluminum oxide membranes (shown in Fig. 2) or nanoimprints supplied by ThunderNIL Srl (in Fig. 3).

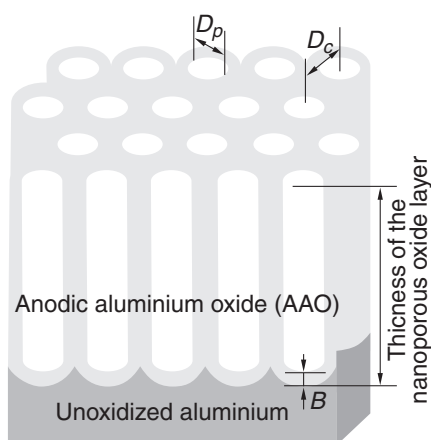


Fig. 2. Ideal structure of anodic aluminum oxide [2].

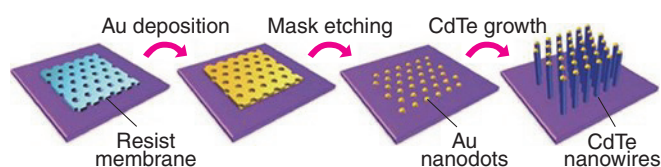


Fig. 3. CdTe nanowires growth using ThunderNIL’s nanopatterned resists.

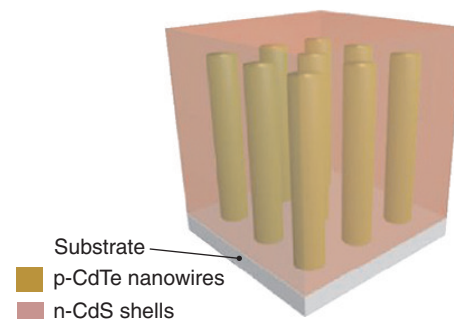


Fig. 4. p-CdTe nanowires embedded in a n-CdS thin film.

Once obtained the templates, different techniques relating the nanostructures growth (sublimation, VLS, CSS, sputtering, spin coating) will be explored.

The nanostructures so obtained will be characterized via XRD, SEM, UV-UVS-IR. It is the aim to then fabricate and test working solar cell devices from the nanowire materials via impedance analysis, current-voltage, capacitance voltage, PV performance (Air Mass 1.5).

Our goal is to demonstrate that is possible to manufacture high performant and cost effective CdTe nanostructured solar cells (as in Fig. 4).

References

- [1] M.A. Green, *et al.* *Progress in Photovoltaics* 25.NREL/JA-5J00-68932 (2017)
- [2] W.J. Stepniowski, and M. Salerno. *Manufacturing Nanostructures*, 321–357 (2014).

InGaAs nanowires grown on GaAs nanomembranes by MBE

M. Friedl¹, A. Balgarkashi¹, L. Francaviglia¹, S. Marti-Sanchez², L. Güniat¹, W. Kim¹, V.G. Dubrovskii³, J. Arbiol^{2,4}, A. Fontcuberta i Morral¹

¹ Laboratory of Semiconductor Materials, École Polytechnique Fédérale de Lausanne, Switzerland

² Catalan Institute of Nanoscience and Nanotechnology (ICN2), CSIC and BIST, Campus UAB, Bellaterra, 08193 Barcelona, Catalonia, Spain

³ ITMO University, Kronverkskiy pr. 49, 197101 St Petersburg, Russia

⁴ICREA, Pg. Lluís Companys 23, 08010 Barcelona, Catalonia, Spain

By growing nanostructures along specific crystalline directions, defect formation can be suppressed [1,2]. Using such an approach, defect-free GaAs nanomembranes have previously been obtained in our group by MBE. The resulting nanostructures have a pristine crystal structure, as demonstrated by very sharp exciton emission [3].

Their perfect crystal structure makes such structures favourable for optical devices. In this work, we looked at extending the functionality of these GaAs nanomembranes to other materials by growing InAs after the growth of GaAs, thus yielding InAs and InGaAs nanowires on top.

GaAs nanomembranes were grown by molecular beam epitaxy (MBE) and followed by the deposition of InAs [4]. We find that the InAs accumulates at the top vertex of the nanomembranes and forms a nanowire, as depicted in Figure 1a. The interface with the GaAs membrane is intermixed in the form of InGaAs, becoming pure InAs in the thicker regions. The nanowires were then analysed by various approaches, including Raman spectroscopy (shown in Fig. 1b), cathodoluminescence (CL) spectroscopy, atomic resolution scanning transmission electron microscopy (AR-STEM) and theoretical modelling of their shape.

It was found that the nanowire shape is exactly the one dictated by strain and surface energy minimization of the system, leading to an aspect ratio that is well-described by theoretical predictions. Analysis by Raman then shows a shift of the InAs LO-phonon mode which matches a $\sim 3\%$ compressive strain in the nanowire. This was then verified by geometrical phase analysis (GPA) in AR-STEM. With CL spectroscopy on InGaAs nanowires we observe a sharp exciton emission from GaAs nanomembranes combined with a low-energy shoulder close to 900 nm attributed to the InGaAs region. This low-energy shoulder is attributed to InGaAs emission and was used to then map out regions of InGaAs on the sample.

References

- [1] C.-Y. Chi *et al.*, *Nano Lett.* **13**, 2506 (2013).
- [2] G. Tutuncuoglu *et al.*, *Nanoscale.* **7**, 19453 (2015).
- [3] Z. Yang *et al.*, *Nano Lett.* **17**, 2979 (2017).
- [4] M. Friedl, V.G. Dubrovskii *et al.*, *Nano Lett.* (2018). Just accepted, DOI: 10.1021/acs.nanolett.8b00554

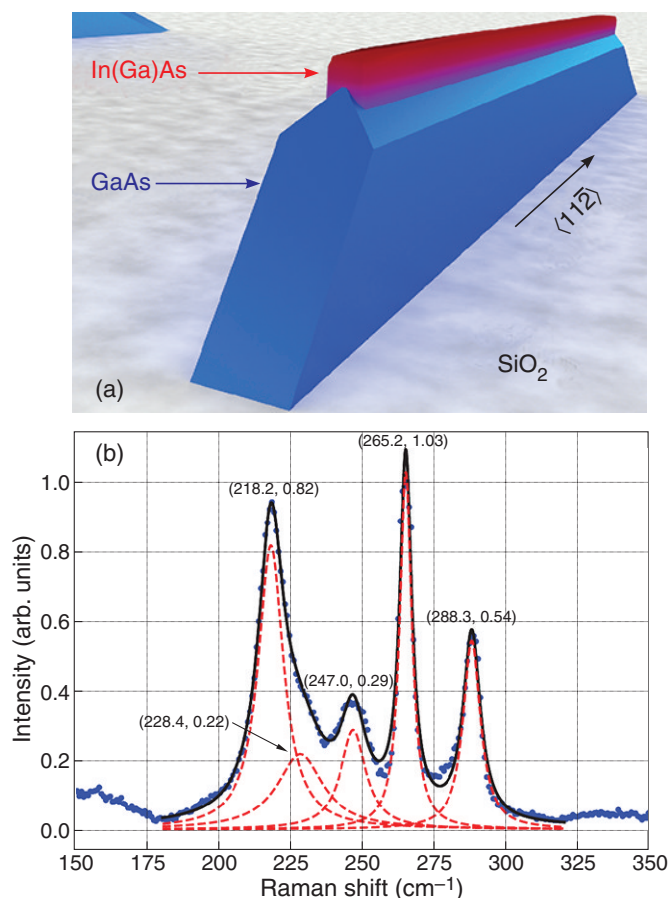


Fig. 1. (a) Depiction of a GaAs nanomembranes with InGaAs nanowire on top. (b) Raman spectrum from the nanowire structure showing contributions from both InAs and GaAs, as well as a strain-shifted InAs LO mode.

Large area single crystal ZnO nanowires grown on ALD seed layers

A. Galan^{1,2}, A.J. Gallant¹, A. Fontcuberta i Morral³, F. Alkhalil⁴, D.A. Zeze¹, D. Atkinson²

¹ Department of Engineering, Durham University, South Rd, Durham, DH1 3LE, UK

² Department of Physics, Durham University, South Rd, Durham, DH1 3LE, UK

³ Laboratoire des Matériaux Semiconducteurs, Institut des Matériaux, Ecole Polytechnique Fédérale de Lausanne, CH-1015 Lausanne, Switzerland

⁴ Pragmatic Printing, Sedgefield, NETPark TS21 3FF

Zinc oxide is a direct wide bandgap semiconductor (3.37 eV) with a high exciton binding energy (60 meV). Among the many different morphologies on that ZnO can be synthesized (nanoflowers, nanobelts, nanodisks¹), nanowires (NWs) are one of the most interesting due to their high aspect ratio and surface area. ZnO nanowires have many different applications such as solar cells² or nanosensors³ due to their electronic and optical properties. For this type of real world applications, nanowires have to be grown on large areas while maintaining high quality and uniformity.

This work describes a low cost, low temperature, large area route to synthesize high quality single crystal ZnO nanowires. These were synthesized using a two-step method. A ZnO seed layer was deposited using Atomic Layer Deposition (ALD). Then, chemical synthesis was carried out to grow ZnO NWs seeded by the ALD-deposited thin film. The specifics of these processes are discussed later. The combination of these two techniques leads to the growth of large area nanowire arrays. This process is low temperature and cheaper compared to traditional techniques used to grown NWs such as MBE or CVD: these techniques require ultra-high vacuum and/or high temperatures (600°C or more). This process only need up to 300°C for the ALD and 90°C for the chemical synthesis. Furthermore, this process does not require a catalyst and the solvent used for the chemical synthesis is water. As shown, the fabrication on NWs by ALD and chemical synthesis is an effective way to obtain nanowires.

ALD is a thin film deposition technique based on self-limiting chemical reactions. It is characterized by its ability to deposit ultra-thin films (through stacking of atomic or molecular layers from precursors) with conformal surface coverage and composition control [4]. The working principle is the pulsing of different precursors (diethyl zinc, DEZ, and water in this case) separately, under a constant flow of nitrogen gas. The precursors are pulsed alternatively and, in between each precursor pulse, there is a purge time when only nitrogen flows. In this process, each precursor will chemisorb to the substrate, forming atomic layers. Thus, an ALD cycle will consist of subsequent pulses and purges of the precursors. The thin films will be formed by the repetition of these cycles. It is vital to have a control over the different properties of the film (composition, roughness, thickness) as this influences the nanowires that can be grown with the desired properties. These film properties are controlled by tuning various parameters such as deposition temperature, number of cycles or the pulse and purge times.

The chemical synthesis involves dissolving an equimolar amount of $Zn(NO_3)_2 \cdot 6H_2O$ and hexamethylenetetramine (HMTA) in DI water and submerging the substrate an ALD film on it. Parameters, such as reagent concentration and syn-

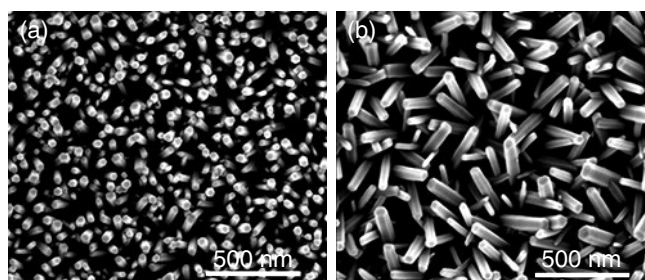


Fig. 1. Top-view SEM images of nanowires grown on thin films deposited with a different number of cycles a) TF280-150, b) TF280-500. The rest of the film deposition and NW synthesis parameters remained the same for both.

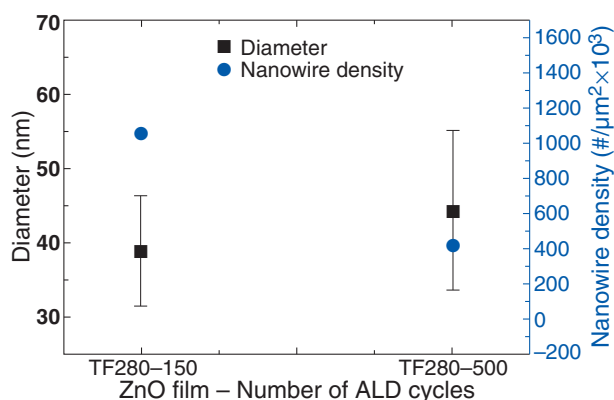


Fig. 2. Comparison of nanowire diameter and density for the samples TF280-150 and TF280-500.

thesis time, can be modified to control the length and diameter of the grown nanowires.

Figure 1 shows an example of the tunability of this process. Here, two samples are shown by ALD films where the number of ALD cycles was 150, Fig. 1(a), and 500, Fig. 1(b). All other parameters remained unchanged. It is shown that an increase in the number of cycles leads to more randomly oriented nanowires, which is attributed to an increase in the ALD film roughness.

Figure 2 shows a comparison of the size and density of the previously shown nanowires where those vertically aligned were smaller in diameter. The smaller diameter coupled with the vertical alignment led to a higher density of NWs per unit area.

Figure 3 shows how changing the chemical synthesis conditions affects the nanowire growth, mainly their diameter and length. Figure 3(a) refers to sample a sample with synthesis time of 2 hours and concentration of 50 mM and Fig. 3(b) was grown for 6 hours with a concentration of 25 mM. The first

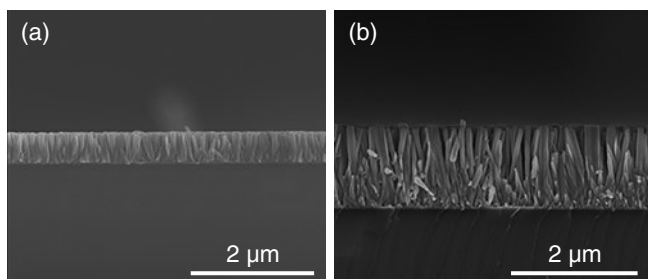


Fig. 3. Cross-section images of the nanowire samples (a) TF250 2h-50 mM and (b) TF250 6h-25 mM, grown under different synthesis conditions in terms of synthesis time (2 or 6 hours) and reagent concentration (25 and 50 mM)

sample has a lower synthesis time while having higher concentration. This indicates that higher concentrations lead to higher diameter nanowires. At the same time, increasing the synthesis time leads to longer NWs.

This process produces high quality nanowires. This is evidenced in Fig. 4(a), where a typical TEM image of the ZnO nanowires obtained by this method is shown. This TEM micrograph demonstrates that there are no defects along the whole wire. Figure 4(b) shows the diffraction pattern of the nanowires, which indicates that the NWs grow in the (002) direction. These results clearly demonstrate that their crystal structure is wurtzite. In brief, the ZnO nanowires produced by this the chemical bath deposition method exhibit single crystal wurtzite phase.

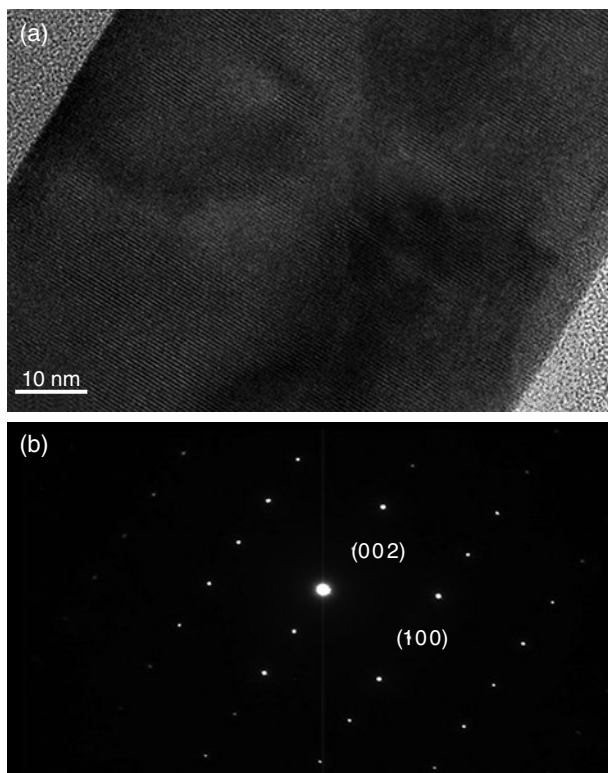


Fig. 4. (a) TEM image of the nanowires and (b) diffraction pattern of same nanowires.

Acknowledgements

This project has received funding from the European Union's Horizon 2020 research and innovation programme under the Marie Skłodowska-Curie grant agreement No/ 722176. The authors also thank Dr. Michael Cook for his help with the ALD.

References

- [1] Y.-B. Hahn, *Korean J. of Chemical Engineering*, **28**(9) 1797–1813 (2011).
- [2] S. Li, P. Zhang *et al*, *Nano Research*, **10**(3) 1092–1103 (2016).
- [3] C.H. Tan *et al*, *Sensors and Actuators B: Chemical*, **248** 140–152 (2017).
- [4] R.W. Johnson, *et al*, *Materials Today*, **17**(5) 236–246 (2014).

Lasers, sources of single photons and entangled photon pairs based on quantum dot in nanowire system

Z.M. Lashkami, *E. Gholami*

Department of Physics, Zanjan University, Zanjan, Iran

Long-distance quantum communication is one of the prime goals in the field of quantum information and with information encoded in the quantum state of photons, existing telecommunication fiber networks can be effectively used as a transport medium for routing photonic qubits, make quantum correlations and entanglement between different nodes. Quantum networks can interconnect remote quantum processors, and links between different architectures to increase net computational power.

Polarization entangled photons suffer from decoherence in optical fibers due to polarization mode dispersion. This effect results in the wavelength and time-dependent splitting of the principal states of polarization with a differential group delay. Thus, the arrival time of the photons carries information about their polarization state causing decoherence.

So, to achieve Long-distance quantum communication, a source of coherent entangled single-photon pairs is required and quantum dots embedded in nanowire waveguides with a controlled shape could serve as an efficient source of single photons and entangled photon pairs for use in quantum cryptography and quantum computing. Quantum information protocols such as quantum teleportation and entanglement swapping use entangled photons to enable long-distance distribution of entanglement through quantum repeaters.

Our goal is to develop and design a prototype of a laser of which the emitted photons would be anti-bunched and violate Bell's inequality by at least 5 standard deviations. Next step could be making them manufacturable by reducing costs.

Nanowires as the object of patenting: landscaping

V. Kaliteevskii, L. Chechurin

Lappeenranta University of Technology

Abstract. Nanowires with the right selection of materials and the overall design of the system begin to possess unique properties. The study and investment in the field of nanowires is very popular and rapidly developing from the phase of laboratory research into the industrial production. This process has a clear support in the form of an increase in the number of patent applications. Analyzing patents on a particular topic, one can draw conclusions about trends and try to predict trends in the development of the market. In this work, we do a patent review on the topic of nanowires from the inventive perspective and show the corresponding results of our investigation. This patent landscaping was carried out to find the patterns in the development of the nanotechnology, to build a system of links in the field of approaches to the production, use and application of nanodevices, in particular nanowires, to build a theory in the field of conceptual design of technologies and products based on nano elements. This work answers, what is the most interesting topic for companies about nanowires, what are the potential industrial applications in use of nanowires and what are the development trends of producing of nanowires. The results are provided by usage of literature and patents review and also data-mining approaches and quantitative statistics.

Stationary and transient optical measurements in semiconductor nanowires

A.K. Sivan¹, L. Di Mario², S. Rubini³ and F. Martelli¹

¹ IMM-CNR, via del fosso del cavaliere 100, Rome, Italy

² ISM-CNR, via del fosso del cavaliere 100, Rome, Italy

³ IOM-CNR, Basovizza, Trieste, Italy

Semiconductor nanowires (NWs) possess a number of unique properties that make them potential building blocks in electronic and optoelectronic devices [1]. In order to use NWs in optoelectronic devices, it is necessary to have a deep understanding of the carrier dynamics and optical properties of the NWs. In this work we present a study of carrier dynamics and other optical properties in semiconductor NWs of different materials. We investigate the influence of the presence of metallic nanoparticles on the NW sidewalls on the static and transient optical properties of ZnSe NWs grown by MBE at low temperature (300–350 °C) for better optical properties [2]. In particular, the nanowires were decorated with silver NPs by thermal dewetting. The presence of the localized surface plasmon resonance produced by the NPs at energy close the ZnSe bandgap has a strong impact on the optical properties of the NWs.

In Fig. 1a, the low temperature PL of bare ZnSe NWs (red line) shows a broad band showing some shoulder that we attribute to a donor-acceptor pair (DAP) band, as deduced by its temperature dependence. The Ag decorated NWs show instead a well-structured band composed of four peaks (black curve of Fig. 1a) separated by the LO phonon energy, as confirmed by the Raman spectrum of the same sample (Fig. 1b). The Ag NPs also induce the observation of near-band-edge emission that includes bound- and free-exciton recombination.

We also study the fast-transient absorption spectroscopy (FTAS) of InGaAs/GaAs core shell structures grown using MBE on a GaAs substrate, using a pump-probe technique. The core shell structure consists of a core (InGaAs) with a smaller band gap surrounded by a thin shell with a larger band gap (GaAs) material. These core-shell structures provide intense PL, and the larger gap material acts as a carrier reservoir in the system [3]. The nanostructures were mechanically transferred onto a transparent substrate (quartz) to enable FTAS in transmission mode. The FTAS spectra show absorption bleaching at the energies corresponding to the band gaps of the two materials. The analysis of the carrier-phonon scattering and of many-body effects, like band gap renormalization is ongoing.

Finally, we also present the FTAS of Si NWs grown on Si and quartz substrates. Though Si has been the centre of many investigations, we use the method of ultrafast pump-probe methods to study the carrier dynamics in Si nanowires to have a better understanding of the direct and indirect band transitions. In particular, we will show that the absorption bleaching at the direct gap of silicon can be observed also for pump energies well below the relative value of 3.3 eV, because of the excitation of electrons from the valence band to the indirect band states of silicon. Combining the pump probe experiments performed with energies above and below 3.3 eV we can hence separate the electron and hole contributions to the bleaching relaxation.

Acknowledgement

This work has received funding from the Horizon 2020 program of the European Union for research and innovation, under grant agreement No. 722176 (INDEED).

References

- [1] R. Agarwal & C. Lieber, *Appl. Phys. A* **85**, 209 (2006).
- [2] Lin Tian *et al.*, *Phys. Rev. B* **94** 165442 (2016).
- [3] F. Jabeen *et al.*, *Appl. Phys. Letters* **93**, 083117 (2008).

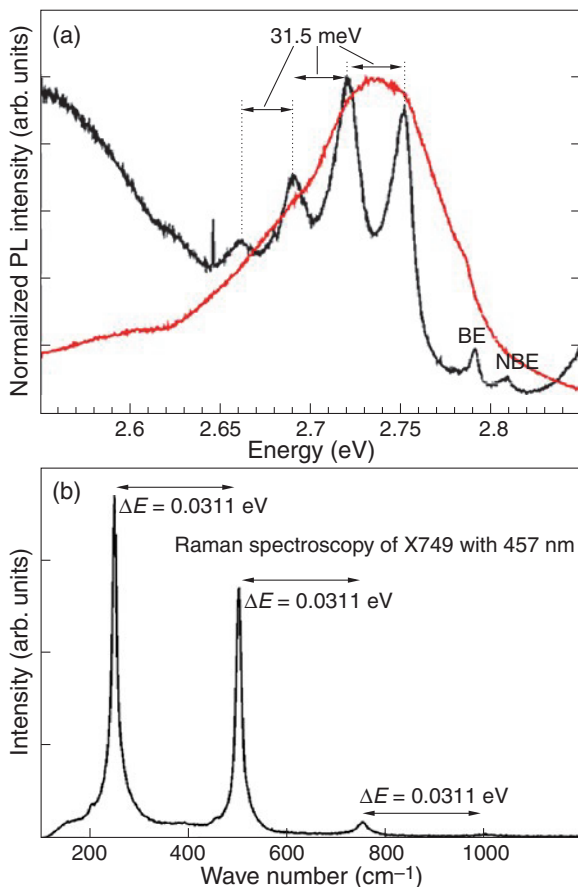


Fig. 1. (a) Normalized PL intensities of ZnSe NWs with (black) and without (red) Ag nanoparticles at 10K; (b) Raman spectroscopy of ZnSe NWs.

Ordered GaAs nanowire arrays on silicon and dopant incorporation studies

W. Kim¹, V.G. Dubrovskii², J. Vukajlovic-Plestina¹, G. Tuñuñoğlu¹, L. Francaviglia¹, D. Mikulik¹,
E. Stutz¹, L. Guñiat¹, H. Potts¹, M. Friedl¹, J.-B. Leran¹ and A. Fontcuberta i Morral¹

¹ Laboratory of Semiconductor Materials, École Polytechnique Fédérale de Lausanne, Lausanne, Switzerland

² ITMO University, Kronverkskiy pr. 49, 197101 St Petersburg, Russia

Inherent small dimension of interfaces enables the nanowire (NW) structures to play an important role in monolithic integration of III-V semiconductor materials with silicon electronic platform. In this work, we present in-depth studies on self-assisted GaAs NW arrays grown on silicon by molecular beam epitaxy. Controlling morphological and structural properties of NWs is essential for their device applications. We analyze the size distributions of ordered NWs at the initial stage of the growth and find that the NW size uniformity can be drastically improved by increasing supersaturation of the vapor phase [1]. We also demonstrate the existence of two stable contact angles of the gallium droplet on top of GaAs NWs, which enables the droplet shape engineering by tuning the V/III flux ratio during growth. The optimized growth procedure yields highly uniform ultrathin (only 10 nm in radius) one-dimensional GaAs nanoneedle (NN) structures on top of GaAs NWs [2]. Finally, we study the incorporation of silicon dopant into the nanowire core and shell. We discuss the growth and doping mechanism and compare our findings to the previous results obtained for self-assisted GaAs nanowires [3,4].

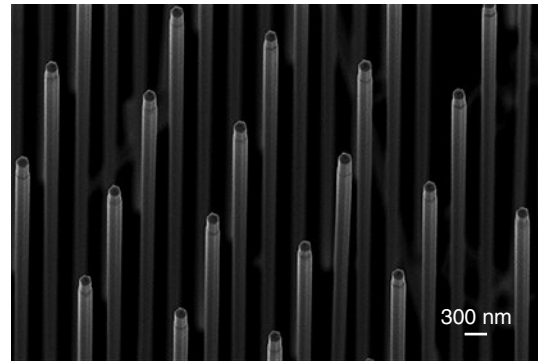


Fig. 1. SEM images of Si-doped GaAs NWs in ordered arrays with an array pitch of 1400 nm. The scale bar corresponds to 300 nm.

References

- [1] J. Vukajlovic-Plestina, W. Kim, V.G. Dubrovskii *et al*, *Nano Letters* **17**, 4101–4108 (2017)
- [2] W. Kim, V.G. Dubrovskii *et al*, *Nano Letters* **18**, 49–57 (2018)
- [3] C. Colombo *et al* *Appl. Phys. Lett.* **94**, 173108 (2009).
- [4] J. Dufouleur *et al*, *Nano Letters* **10**, 1734 (2010).

Turning the growth direction of GaAs NWs during self-catalyzed MBE

E. Koivusalo, T. Hakkarainen, M. Guina

Optoelectronics Research Centre, Tampere University of Technology, Tampere, Finland

The NW geometry can be extended beyond typical 1-dimensional design by turning the NW growth direction as previously demonstrated for MBE grown catalyst-free InAs(Sb) [1] and Au catalyzed InP NWs [2], as well as for MOVPE grown Au-catalyzed GaAs [3] and InP [4] NWs. Control over the NW growth direction could be utilized for example to form nanocross based quantum devices [5]. Moreover, L-shaped nanostructures with broken symmetry could be used for chiral photonics and sensing [6]. All these works rely on controlling the position and properties of the catalyst droplet during NW growth. We have previously demonstrated MBE growth of self-catalyzed GaAs NWs with sub-Poissonian length distributions [7] indicating a high level of catalyst control and uniformity in our growth method.

In this work, we present a simple in-situ method for changing the growth direction of self-catalyzed GaAs NWs with a 100% yield. After 20 min of vertical NW growth we shut all the fluxes and anneal the sample. This reshapes the NW tip and NW-droplet interface dropping the Ga droplets towards one of the $\langle 110 \rangle$ sidefacets of the NW. After the annealing, the NW growth is resumed forming horizontal kinks along one of the $\langle 112 \rangle$ directions. The growth is pinned by a single horizontal twin plane extending throughout the horizontal part in otherwise defect-free zinc blende structure. However, when the NW growth conditions are changed another slightly downward pointing population forms towards one of the $\langle 111 \rangle_B$ directions 109.5° from the original $\langle 111 \rangle_B$ growth direction. We discuss the steps for forming these new NW structures, effect of growth conditions to the yields of different types of horizontal growth and the morphological changes involved in each step, based on statistical analysis of the NW morphologies by SEM and microstructure of the NW tip and droplet-NW interface revealed by HR-TEM.

In particular, the main focus of this work is on systematically analysing the effects of NW density, and growth conditions of the horizontal part on the yield of the horizontally grown kinks. Samples with three different, NW densities, annealing times and V/III ratios were grown to analyse these effects. All three parameters are found to affect the morphologies of resulting horizontal part. The annealing time is found to be the most effective parameter achieving 100% yield for single population of horizontal structures.

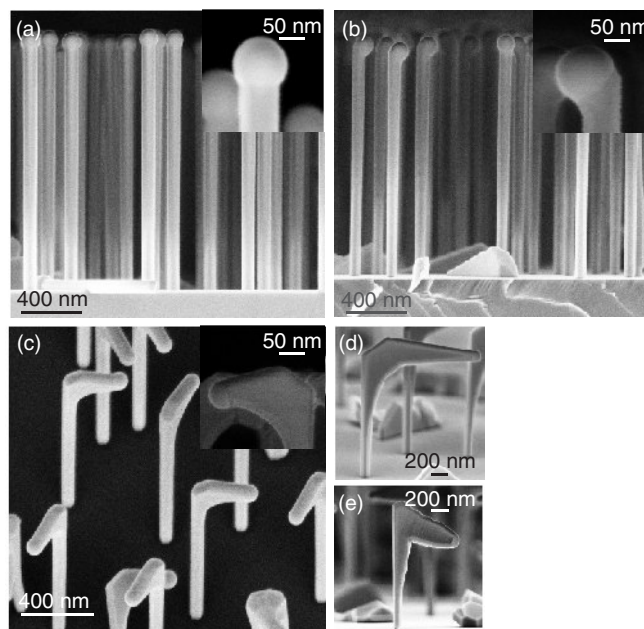


Fig. 1. Steps of turning the NW growth direction and different types of the horizontal part. Regular NWs grown for 20 min and cooled down rapidly after the growth without any fluxes (a). Annealing reforms the NW top facets (b). Continuing the growth after the annealing forms a 100% yield of kinked NWs (c). Modification to growth conditions yields to two populations of kinked NWs (d) and (e). Scale bars (a–c) 400 nm, insets 50 nm, (d–e) 200 nm.

References

- [1] H. Potts, *et al.*, *Nanotechnology* **28**(5) 054001 (2017).
- [2] J. Wang, *et al.*, *Nano Lett* **13**(8) 3802–3806 (2013).
- [3] X. Yuan, *et al.*, *Adv Mater* **27**(40) 6096–6103 (2015).
- [4] A. Kelrich, *et al.*, *Nano Lett* **16**(4) 2837–2844 (2016).
- [5] S. Gazibegovic, *et al.*, *Nature* **548** 434–438 (2017).
- [6] E. Petronijevic, *et al.*, *Opt Express* **25**(13) 14148–14157 (2017).
- [7] E. Koivusalo, *et al.*, *Nano Lett* **17**(9) 5350–5355 (2017).

Nucleation limited composition of ternary nanowires

E.D. Leshchenko¹, M. Ghasemi^{1,2}, V.G. Dubrovskii³, J. Johansson¹

¹ Solid State Physics and NanoLund, Lund University, Box 118, 221 00 Lund, Sweden

² Physics Department, Persian Gulf University, Box 7513613817 Booshehr, Iran

³ ITMO University, Kronverskiy pr. 49, 197101 St Petersburg, Russia

The nanowire composition plays a key role in bandgap engineering and sensing properties of nanoscale nanowire-based devices. The ability to fully control the composition of ternary nanowires is impossible without understanding of the growth process. However, in spite of comprehensive research efforts devoted to nanowire growth modeling [1–3], there is still no complete description of nanowire growth from quaternary alloys. In this respect, we present an analytical approach for tuning the nanowire composition and compare our calculations with the results of an equilibrium thermodynamic model. Here we focus on the vapor-liquid-solid growth of ternary nanowires of III-V semiconductor compounds in the nucleation-limited regime. Several ternary systems are considered including In-Ga-As-Au, Al-Ga-As-Au, In-Ga-Sb-Au and In-Sb-As-Au. In the current contribution special attention is paid to analysis of liquid-solid composition dependencies for different concentrations of group III element and, in particular, to comparison of self-catalyzed and Au-catalyzed nanowire growth (Fig. 1(a)). Moreover, within the model a miscibility gap where the formation of the homogeneous solid solution is thermodynamically forbidden is obtained (Fig. 1(b)).

Acknowledgement

EDL and JJ gratefully acknowledge financial support from the European Union’s Horizon 2020 research and innovation program under the Marie Skłodowska-Curie grant 722176 (project acronym INDEED).

References

- [1] J. Johansson and M. Ghasemi, *Phys. Rev. Materials* **1** 040401 (2017)
- [2] F. Glas, *Cryst. Growth Des* **17** 4785–4794 (2017)
- [3] V.G. Dubrovskii, A.A. Koryakin and N.V. Sibirev, *Materials and Design* **132** 400–408 (2017).

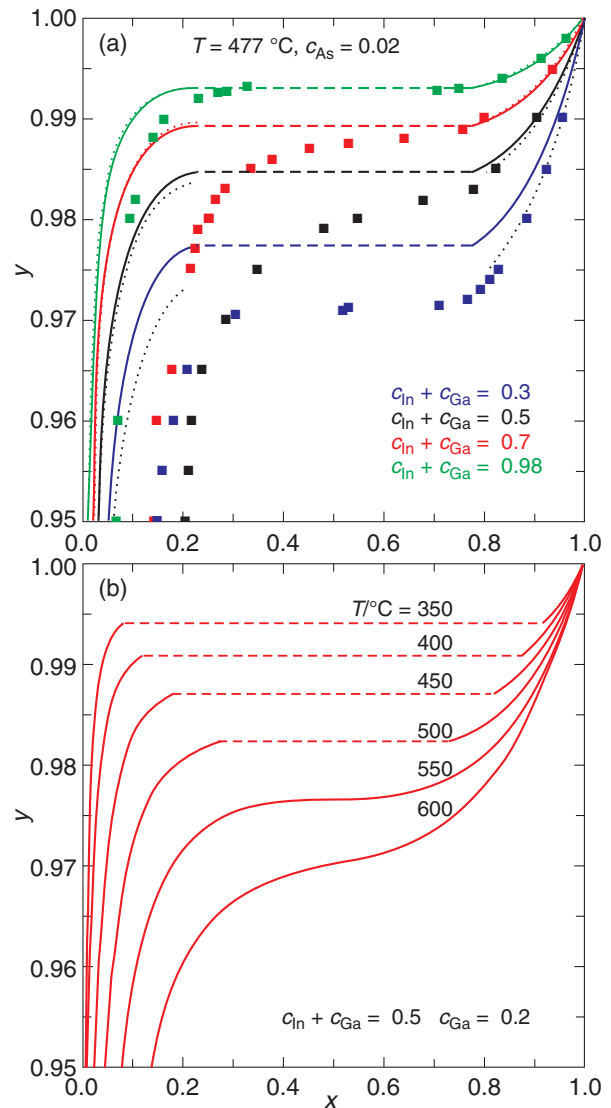


Fig. 1. Analytically calculated liquid-solid composition dependencies for different concentrations of group III element (a) and temperatures (b) for In_xGa_{1-x}As nanowires.

Controlling the surface morphology of III-V semiconductor nanowires

N. Peric¹, A. DiazAlvarez¹, T. Xu^{1,2}, M. Schnedler³, I. Lefebvre¹, G. Patriarche⁴, J.P. Nys¹, S.R. Plissard⁵, P. Caroff⁶, M. Berthe¹, H. Eisele⁷, R.E. DuninBorkowski³, Ph. Ebert³, B. Grandidier¹

¹ Univ. Lille, CNRS, Centrale Lille, ISEN, Univ. Valenciennes, UMR 8520 – IEMN, F-59000 Lille, France

² Key Laboratory of Advanced Display and System Application, Shanghai University, 149 Yanchang Road, Shanghai 200072, People's Republic of China

³ Peter Grünberg Institut, Forschungszentrum Jülich GmbH, 52425 Jülich, Germany

⁴ Laboratoire de Photonique et de Nanostructures (LPN), CNRS, Université Paris-Saclay, route de Nozay, 91460 Marcoussis, France

⁵ Laboratoire d'Analyse et d'Architecture des Systèmes (LAAS), CNRS, Université de Toulouse, 7 Avenue du Colonel Roche, 31400 Toulouse, France

⁶ School of Physics and Astronomy, Cardiff University, Cardiff, Wales CF24 3AA, UK

⁷ Institut für Festkörperphysik, Technische Universität Berlin, Hardenbergstrasse 36, 10623 Berlin

Advances in the growth of nanowires allow for the fabrication of complex crystal structures, which otherwise are unstable and hence cannot be achieved in the bulk. As the geometry of these one-dimensional (1D) systems leads to a very high surface-to-volume ratio a good understanding of the surface properties is essential, since tuning their properties might offer additional degrees of freedom in the fabrication of (1D) heterostructures [1,2]. Here, with the use of scanning tunneling microscopy we will focus on III-V semiconductor nanowires and investigate the morphology and electronic structure of their sidewalls as a function of the growth conditions or the post-growth conditions [3].

In particular we will show how a lateral growth mode leads to the formation of $\langle 112 \rangle$ -oriented steps on the sidewalls of zincblende nanowires. Such steps are at the origin of a local ordering in alloy compounds that was directly observed on the sidewalls of InAsSb nanowires, for example. It is caused by the repulsive interaction between Sb atoms, leading to the incorporation of Sb atoms along specific crystallographic directions [4].

We will also discuss methods to recover clean and well-ordered sidewalls once the nanowires have been transferred through air [5,6]. Among the existing methods we will emphasize on the protection of the sidewalls of nanowires with an amorphous As capping layer. We will show that the sublimation of the capping layer produces sidewalls with different morphologies depending on the chemical composition of the nanowires and the nature of the seed particles. As seen in Fig. 1 the sidewall of an InAs nanowire appears with small holes, whereas the sidewall of a GaAs nanowire shows one atomic step height terraces. We will explain the origin of this morphology change that is related to the energy formation of point defects at the surface of the nanowires.

As the sidewalls of zinc blende nanowires grown along a $\langle 111 \rangle$ direction exhibit $\{110\}$ facets, these sidewalls are naturally passivated. We will take advantage of the passivation to probe the electronic structure of nanowires with multiple shells. Such a configuration is particularly appealing to measure the band offset across a radial heterointerface and we will give rules to determine, with tunneling spectroscopy, the band discontinuities of a wide range of other 1D heterostructures [7].

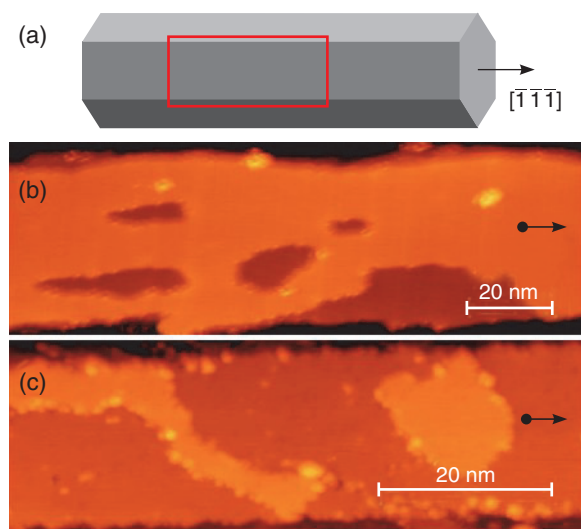


Fig. 1. (a) Schematic of a $[\bar{1}\bar{1}\bar{1}]$ grown III-V semiconductor nanowire. The red rectangle indicates the area of a sidewall that is characterized with scanning tunnelling microscopy. (b) STM image of the sidewall of a self-catalyzed InAs nanowire. (c) STM image of the sidewall of a self-catalyzed GaAs nanowire.

References

- [1] X. Guan *et al*, *Nano. Lett.* **16** 2393 (2016).
- [2] W Yang *et al*, *Nano Lett.* **15**, 7574 (2015).
- [3] J. V. Knutsson *et al*, *ACS Appl. Mater. Interfaces* **7**, 5748 (2015)
- [4] M Schnedler *et al* *Phys. Rev. B* **94**, 19536 (216).
- [5] J.L. Webb *et al*, *Nano Lett.* **15**, 4865 (2015)
- [6] T. Xu, B. Grandidier, in *Semiconductor nanowires: Materials, synthesis, characterization and applications*, edited by J. Arbiol and Q. Xiong, Woodhead, Swaston Cambridge UK (2015), **77** 27734
- [7] T. Xu *et al*, *Appl. Phys. Lett* **17** 11212 (2015).

Growth of advanced functional heterostructures in III-V nanowires

A. Pishchagin, F. Glas, J.-C. Harmand, F. Oehler

Centre de Nanosciences et Nanotechnologies (C2N), CNRS, Université Paris-Sud, Université Paris-Saclay,
91400 Marcoussis, France

Semiconductor nanowires, with diameters of a few tens of nanometers and lengths up to several microns, are nowadays commonly fabricated from a large range of semiconductor materials. The remarkable physical properties of these objects open large prospects of original applications, some of which have already been demonstrated. However, their full potential will only be achieved if their physical properties can be precisely tailored. In addition to controlling the geometry, crystal structure and doping of the nanowires, it is necessary to know how to obtain regular arrays of identical nanowires and how to modulate properties locally to confer novel functionalities of each nanowire.

Such novel functionalities could be obtained in particular by achieving quantum confinement in nanowires. For GaAs, this requires that at least one dimension be below about 25 nm. We aim to reduce the nanowire diameter within this range. However, due to several reasons such as difficulties in obtaining very small droplets on the substrate or avoiding radial growth, fabricating very thin nanowires by the vapor-liquid-solid technique is still a challenge.

One of the ways of obtaining a high yield of thin III-V nanowires is to interrupt and resume the growth during the epitaxy process. This technique allows one to fabricate thin nanowires (nanoneedles) on the top on thicker ones [1,2].

This PhD project has just started. Our first goal is to devise a strategy for the fabrication of thin nanowires incorporating a quantum dot type heterostructure on top of a thicker stem. Specifically, we will investigate the growth of self-catalysed GaAs/Ga(As,P) nanowire structures with different configurations. The growth will be performed on patterned SiO_x/Si(111) substrates with pitches from 200 nm to 1 μm. Experiments and modelling will be performed to understand and master the processes occurring on the top of the nanowire stem. The control of the nanowire diameter and of the crystal structure of the insertion as well as the possible exchange of material between nanowires will be investigated. The control of the formation of a shell designed to alter the optical properties of the insertion via strain will be of particular concern. Ultimately, we intend to fabricate uniform arrays of thin nanowires including heterostructures with specific optical properties.

Acknowledgement

This project has received funding from the European Union's Horizon 2020 research and innovation programme under the Marie Skłodowska-Curie grant agreement No. 722176.

References

- [1] G. Priante *et al.*, *Cryst. Growth Des.*, **13**, 3976–3984 (2013)
- [2] W. Kim *et al.*, *Nano Lett.*, **18**, 49–57 (2018)

MBE growth and optical properties of GaN, InN and III-V nanowires on SiC/Si(111) hybrid substrate

R.R. Reznik^{1-4,7}, K.P. Kotlyar¹, I.P. Soshnikov^{1,3,5}, E.V. Nikitina¹, S.A. Kukushkin⁶, A.V. Osipov⁶ and G.E. Cirilin^{1,4,5}

¹ St Petersburg Academic University RAS, Khlopina 8/3, St Petersburg, Russia

² Peter the Great St Petersburg Polytechnic University, Polytechnicheskaya 29, St Petersburg, Russia

³ Institute for Analytical Instrumentation RAS, Rizhsky 26, St Petersburg, Russia ⁴ ITMO University, Kronverkskiy pr. 49, St Petersburg, Russia

⁵ Ioffe Institute, Politekhnicheskaya 26, St Petersburg, Russia ⁶ Institute of Problems of Mechanical Engineering RA S, Bolshoj 6, St Petersburg, Russia ⁷ Department of Engineering, Durham University, Durham DH1 3LE, UK

The nanoheterostructures based on III-nitrides and III-V nanowires (NWs) are of great interest for creating electronic and optoelectronic devices [1]. Works in growing GaN layers on silicon [2] have been very promising recently. However, the lattice misfit of such materials is 17%, which leads to the formation of defects of different nature. It is known that the optoelectronic GaN based devices can operate for a long time without degrading despite the high density linear defects. Nevertheless, to extend the lifetime of optoelectronic devices is necessary to increase the perfection of GaN structures.

In this work, in order to reduce the number of misfit dislocations or to reduce the diameter of NWs a nanometer (about 50 nm) buffer layer of SiC was used. It is grown on Si by solid-phase epitaxy, which provides extremely low values of the density of misfit dislocations, since the difference in the lattice parameters is only 3%, and also, instead of a planar layer, growth GaN nanowires (NWs), which can radically reduce the density of structural defects. In addition to nitrides, III-V nanowires such as GaAs, AlGaAs and InAs have been successfully grown by molecular beam epitaxy on such hybrid substrates. In this case, it was assumed that a huge lattice mismatch between SiC and III-V materials would lead to a significant reduction in NWs diameter. Due to this, the quantum-dimensional effects of the material can be manifested more clearly.

Growth experiments are carried out using Riber Compact 12 and 21 MBE setup equipped with the effusion Ga, Al, In, As cell and the nitrogen source. Growth time of GaN NWs was 16 hours.

After the growth, the samples are studied by applying the scanning electron microscopy (SEM) and low-temperature photoluminescence (PL) techniques.

The intensity of radiation grown on SiC buffer layer GaN NWs is more than two times higher than the intensity of the best grown on silicon structures of GaN. This fact leads to the conclusion that grown in this work structures have fewer defects compared with GaN NWs on silicon substrate, which, in its turn, have few defects. This is caused by a smaller lattice constant mismatch between GaN and SiC as compared with GaN and Si.

Moreover, a possibility of A³B⁵ GaAs, AlGaAs and InAs nanowires growth on a silicon substrate with a nanoscale buffer layer of silicon carbide has been demonstrated for the first time. The diameter of these NWs is smaller than diameter of similar NWs which were grown on a silicon substrate, because of significant lattice mismatch. In particular, InAs NWs diameter was less than 10 nm. In addition, based on photoluminescence measurements, it was found that, in case of AlGaAs NWs growth on such substrates, complex structure forms due to the self-organized AlGaAs quantum dot with lower composition of aluminum embedded in NWs body.

Because of the considerable mismatch between InAs and SiC, the critical Au droplet diameter is very small, so InAs NWs density turned out to be extremely low. The diameter of such InAs NWs can not accurately determined by means of a scanning electron microscope since NWs oscillate under the electron beam charging. With certainty their diameter as less as 10 nanometers can be evaluated, which is less than the de Broglie wavelength for InAs.

References

- [1] S.J. Pearton, F. Ren, *Adv. Mater.* **11**, 1571 (2000).
- [2] I.G. Aksyanov, V.N. Bessolov, S.A. Kukushkin, *Techn. Phys. Lett.* **34**, 479 (2008).

Structural and transport properties of Be-doped self-catalysed GaAs nanowires grown by molecular beam epitaxy

M.R. Piton^{1,2}, E. Koivusalo¹, S. Suomalainen¹, T. Hakkarainen¹, S. Souto³, H.V.A. Galeti⁴, D. Lupo⁵, A.D. Rodrigues², Y.G. Gobato² and M. Guina¹

¹ Optoelectronics Research Centre, Tampere University of Technology, Tampere, Finland

² Physics Department, Federal University of São Carlos, São Carlos-SP, Brazil

³ FZEA/ZAB, University of São Paulo, Pirassununga-SP, Brazil

⁴ Electrical Engineering Department, Federal University of São Carlos, São Carlos-SP, Brazil

⁵ Electronics and Communications Engineering, Tampere University of Technology, Tampere, Finland

Semiconductor nanowires (NWs) have been research target for a wide range of nanoscale optoelectronic devices, such as lasers, sensors lightemitters etc In particular the growth of III-V NWs by molecular beam epitaxy (MBE) yields a good control of structural properties and size distributions The possibility of NWs growth directly on silicon substrates is a promising alternative of III-V materials with the current optoelectronics technology, but a reliable doping procedure without compromising the NWs structural quality is required to achieving competing device performances In this work we present structural optical and transport properties of Bedoped selfcatalysed GaAs NWs grown by MBE. The NWs are grown on pSi(111) substrates using lithographyfree Si/SiO_x templates fabricated by droplet epitaxy and spontaneous oxidation, yielding highly uniform NWs with great control of size and density distributions and majority of Zinc Blende (ZB) crystalline structure [1–3]. Nominal Be doping levels of 2×10^{18} and $2 \times 10^{19} \text{ cm}^{-3}$ of the GaAs NWs was achieved by adjusting the effusion cell temperature according to previous planar growth calibrations carried by Hallmeasurements

Figure 1(a–c) shows lateral SEM images of Bedoped and undoped GaAs NWs The lower Be doping level (Fig. 1c) yielded a slightly broader length distribution with smaller NW diameter and tapering when compared to the other samples HRTEM combined with selected area electron diffraction (SAED) data shows that the bottom part of the NW is composed of several stacking faults and twin planes, which reflects the initial stages of NW growth The centre region was found to be a defect free ZB structure that extends to the top part of the NW with a few stacking faults formation. The NWGa droplet interface presented stacking faults formation from growth termination these results are in well agreement with previous growth f undoped self-catalysed GaAs NWs [2].

Micro-Raman spectroscopy of single NWs transferred to amorphous glass substrates was carried out to investigate the doping level of the NWs by analysis of the reduction of the longitudinal optical (LO) phonon modes. The LO mode suppression for the Be-doped samples is an indicative of dopant incorporation to the NWs lattice due to the screening of this mode caused by an increase in the depletion layer width at the surface of the NWs [4]. The peak labels and positions of the vibrational modes in Fig. 1(d) were related to the undoped sample and are in well agreement to previous reported studies with the transversal optical mode (TO) centered at 268 cm^{-1} and the longitudinal optical (LO) mode at 291 cm^{-1} [5]. A surface optical (SO) mode at 289 cm^{-1} was also observed for the ref-

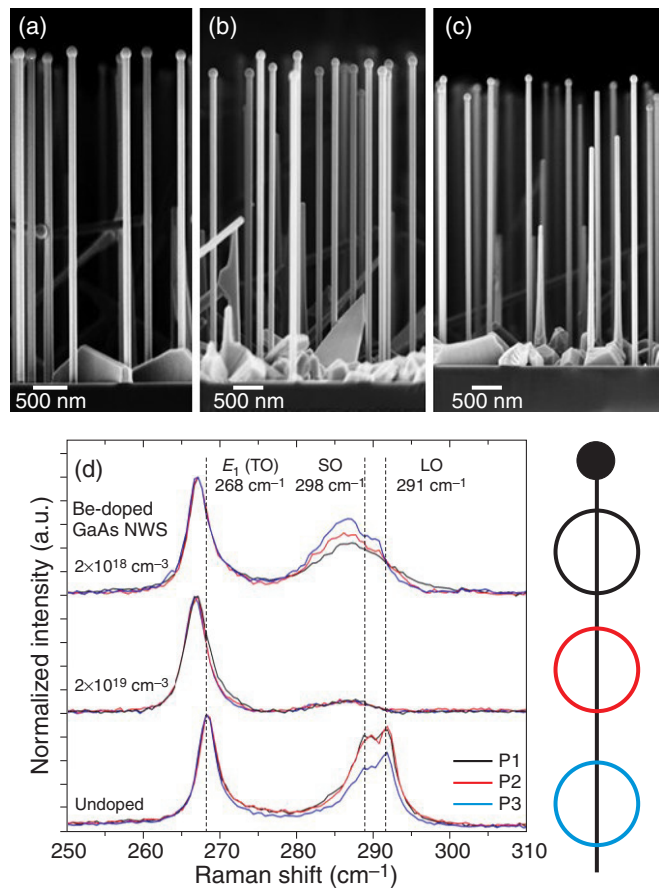


Fig. 1. Lateral SEM images of (a) undoped, (b) $2 \times 10^{19} \text{ cm}^{-3}$ and (c) $2 \times 10^{18} \text{ cm}^{-3}$ Be-doped GaAs NWs. The scale bar is 500 nm. (d) micro-Raman spectra of undoped and Bedoped single GaAs NWs. The dashed lines show TO, SO and LO positions in relation to the undoped NW. The measurements were carried out using a 532 YAG solid state laser excitation with power controlled to avoid heating contributions to the spectra The spot size was $1 \mu\text{m}$. The image on the right of (d) illustrates the positions of the NW from where the spectra were acquired.

erence and $2 \times 10^{18} \text{ cm}^{-3}$ Bedoped sample (286 cm^{-1}), which can be ascribed to size effects [6]. Transport properties were investigated by fabricating standard pGaAs electrical contacts on single GaAs NWs by electron beam lithography and electron beam metal evaporation. An oxide removal and surface chemical passivation steps were performed on the exposed contact area of the NWs prior to metal evaporation. Current voltage

(IV) measurements of undoped and $2 \times 10^{19} \text{ cm}^{-3}$ Bedoped NW are shown in Fig. 2, an SEM image of the Bedoped sample device is also illustrated the geometry was designed in such way to obtain transmission line measurement (TLM) data for both semiconductor and contact resistivity. The difference in IV for same applied bias is a clear evidence of dopant incorporation into the NWs lattice and the IV linearity of the Bedoped sample indicates that ohmic contact was achieved.

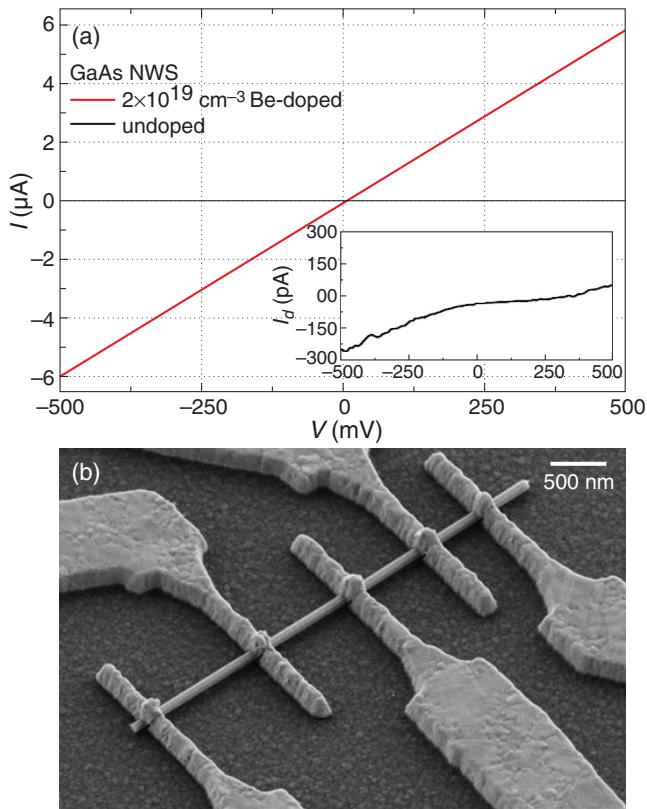


Fig. 2. (a) IV from undoped and $2 \times 10^{19} \text{ cm}^{-3}$ Bedoped GaAs NWs. The inset shows IV from undoped NW in a more suitable current scale. (b) 30° tilted SEM image of device for TLM measurements. The scale bar is 500 nm.

References

- [1] T.V. Hakkarainen *et al.* *Nanotechnology* **26**, 275301 (2015).
- [2] E.S. Koivusalo *et al.* *Nanoscale Research Lett.* **12**, 192 (2017).
- [3] E.S. Koivusalo *et al.* *Nano Lett.* **17**, 5350, (2017).
- [4] O. Salehzadeh *et al.* *Appl. Phys. Lett.* **99**, 282102 (2011).
- [5] I. Zardo *et al.* *Phys. Rev. B* **80**, 245324 (2009).
- [6] D. Spirkoska *et al.* *Nanotechnology* **19**, 435704 (2008).

Preparing nanomaterials based on metals and DNA

P.R. Martínez, B. Horrocks, A. Houlton

Chemical Nanoscience Labs, School of Chemistry, Newcastle University, Newcastle upon Tyne NE1 7RU, UK

The goal of this project is to develop efficient methodologies of assembly using metals and nucleic acids well as templates or as ligands. In that way we could confer properties of technological interest to oligonucleotides. To achieve this goal we will focus on the preparation of coordination polymers using noble metals, such copper, gold or silver and nucleobases as bridging ligands. Studies will then be aimed at integrating these types of coordination motif into DNA structures. This nanomaterials, nanowires, will have incomparable properties in their use as building blocks in the next generation of Nano electronic devices and emerging applications.

DNA is an important biopolymer not only because its ability to store and transfer genetic information but also as a raw material to develop nanoscale materials. There are several reason why DNA is really useful for these materials. Specifically, their use in nanoscale materials arises from the controllable length scale, morphology and self-assembling properties that allows bottom-up fabrication with nanometric precision through programming of sequence. All of this makes think of this biopolymer as a useful molecule in the design of materials. However, the components of DNA have deficiency in electronic/magnetic properties. Thus we will carry out some modifications, like introducing metals into its structure, to solve this problem.

With the objective of promote new routes to carry out nanowire functionality into device technologies in mind, this project will investigate self-assembly of molecular-based nanowires to access conducting single molecules, soft-interfaces and gels and regenerating assemblies.

At present time the synthesis of coordination polymers with the mentioned metal is carried out with ligands modified. In the nucleobases exist several positions where the metal could attach, so to improve the selectivity in the bonding we introduce modified bases (ligandosides) who supply metal-ligand logical sites an able to form specific metal binding [1]. Concretely we use thiol derivatives well-knows in medical sciences.

In particular, we are now using sulphur-containing comparable of an original nucleoside, 6-thioguanosine and 6-thioguanine that react with gold (I) (Fig. 1). Using this stable metal thiolate coordination polymers allow us build motifs to integrate into DNA structures allowing the construction of exquisitely complex nanostructured material that also have properties on demand. The metal base pairs is a powerful tool to build homogeneous and heterogeneous metal complex that can lead to nanomaterials based such as electronic wires and magnetic devices.

One of the first objectives of the project was the preparation and characterization of metal (I) thiolate polymers containing the simple nucleobase. Here, we show coordination polymers based on noble metal/nucleobase in forms suited for nanowire experiments (long fibers), as a result we could get an artificial oligonucleotide suitable for linking DNA through sulphur. The

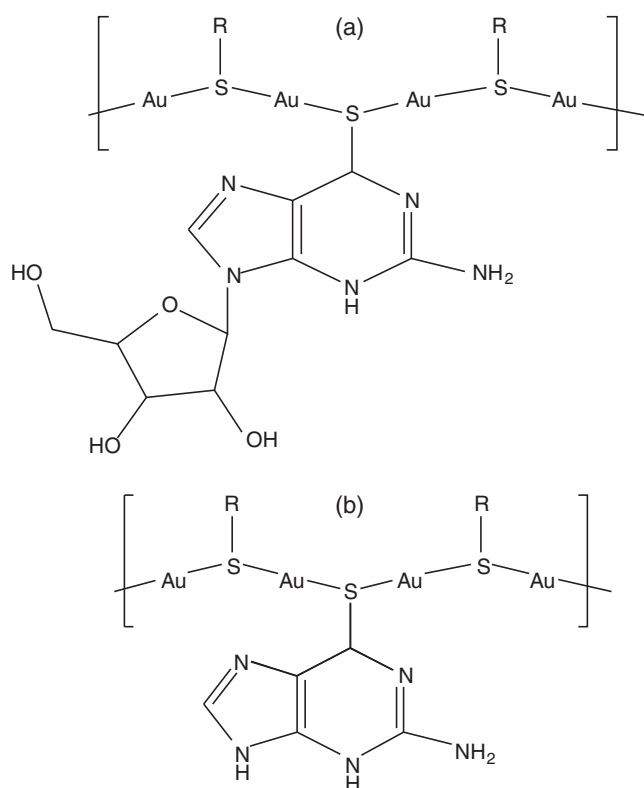


Fig. 1. Sulphur derivatives 6-Thioguanosine (a) and 6-Thioguanine (b), M represents the noble metal in oxidation state +1.

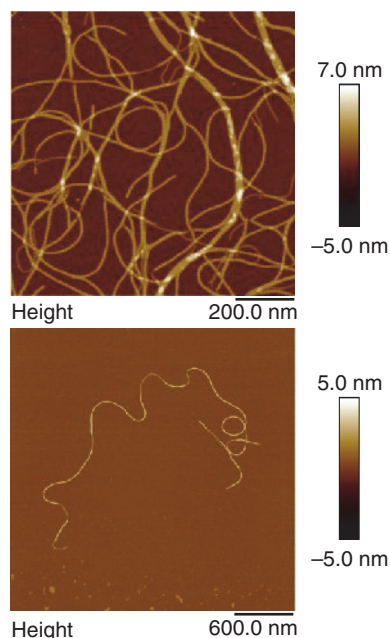


Fig. 2. Fibers formed by the reaction between 6-Thioguanosine and gold (I).

nucleobase used differ only in the presence of sugar molecule in the case of 6-thioguanosine which seems to be key when it comes to obtaining gel or crystalline powder as a product of the reaction with the metal.

The following results using 6-thioguanosine show that after characterization with spectroscopic methods, the emission change when the metal is attached. The fact of obtaining a gel indicates that a molecular framework has been formed and this is confirmed using AFM. As shown (Fig. 2), we can see fibers after the formation of the coordination polymer that are helical. The next step will be obtain crystalline materials with the aim of obtaining further structural information.

Finally we are now preparing metal (I) thiolates nucleotides with extending oligonucleotide sequences which will introduce molecular recognition features and allowing further assembly. In this case we start with oligonucleotides of 16-mer and 2-mer lengths (ThioG-T; ThioG-TTTATGCTCAACTCT). This coordination polymers are interesting because starting from thiolates we could modulate the size of the oligomer and by extension of the resulting polymer. As a result this bonds that holds the strands of DNA together could show us the formation of an extended polymer in the space by interconnected chains, as we see by AFM (Fig 3).

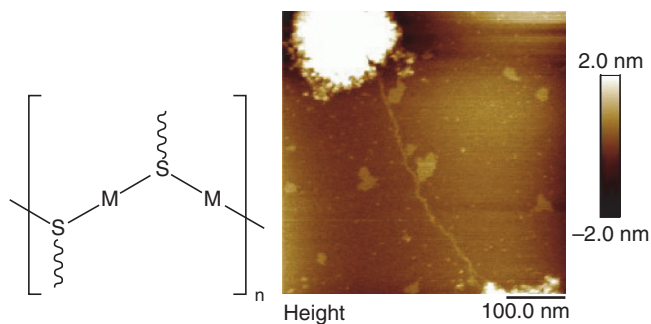


Fig. 3. Formation of 16-mer coordination polymer with gold (I).

References

- [1] A. Houlton, *et al.*, *Nature Communications* **8**, 720 (2017)

Using carbon-nanotube classifiers to diagnose diseases

E. Vissol-Gaudin, A. Kotsialos, C. Pearson, C. Groves, M.C. Petty and D.A. Zeze

Department of Engineering, Durham University, Durham, UK

This paper presents an evolution-in-materio approach that can be followed to produce single-walled-carbon-nanotube/liquid crystal devices able to classify malignant tumors from a series of mammograms. The classification accuracy of the devices is compared to artificial neural network solutions and human diagnosis, indicating that nanomaterials can be used to solve complex computational problems.

Classification is a powerful tool commonly used in data analysis and decision making, where data is categorised according to common features or other pre-defined discriminating criterion. Whilst it is relatively easy to manually classify data or find analytical solutions for small, simple datasets, it becomes near-impossible when their scale and complexity increase. A number of automated methods have been developed to deal with complex classification problems [1]. Supervised learning, for example, can be used to modify the input/output relationship of a 'machine', such as an artificial neural network (ANN), with a search algorithm, until the 'machine' is able to compute correctly a set of known data called training set. The solution, the evolved input/output relationship, must then be able to classify any unknown data it is sent subsequently. However, an ANN requires very large training sets to produce solutions that can be either sub-optimal or over-fitted to this set. It has also been observed that evolutionary algorithms (EAs), commonly used to train ANNs, tend to exploit in their search unknown, intrinsic analogue properties of the basic hardware components upon which they are run, resulting in a loss of efficiency throughout the training process [2].

As an alternative, an evolution in materio (EiM) approach to the production of classifiers has been designed. EiM is a field of research which aims at exploiting the underlying properties of materials to bring them to a computation inducing state [3]. Following this approach, the supervised learning 'machine' is replaced by a material, and the EAs exploit directly the properties of the material their search for a solution. A complex classification problem, illustrated in Fig. 1(a), has been chosen to evaluate EiM solutions. This problem is concerned with discriminating between benign and malignant mammographic masses based on BI-RADS attributes and patient age.

Experimental results obtained by training ANNs to classify the mammographic mass data [6,7] can be compared with EiM results, where the ANNs are effectively replaced by a network of single-walled-carbon-nanotubes (SWCNTs) dispersed in a liquid crystal (LC), and the data is translated into voltage inputs. A SWCNT/LC sample drop-cast on an electrode array is shown in Fig. 1(b). The LC provides a medium within which the SWCNT can move [8], and the composite presents a non-linear current (I)/voltage (V) relationship. Both can be manipulated by an applied electric field, which allows an EA to modify the composite's state by varying this field. The non-linear I/V characteristic of SWCNT/LC samples is important for the successful implementation of EiM computation. In that, semi-conducting nanowires, which inherently exhibit a non-linear

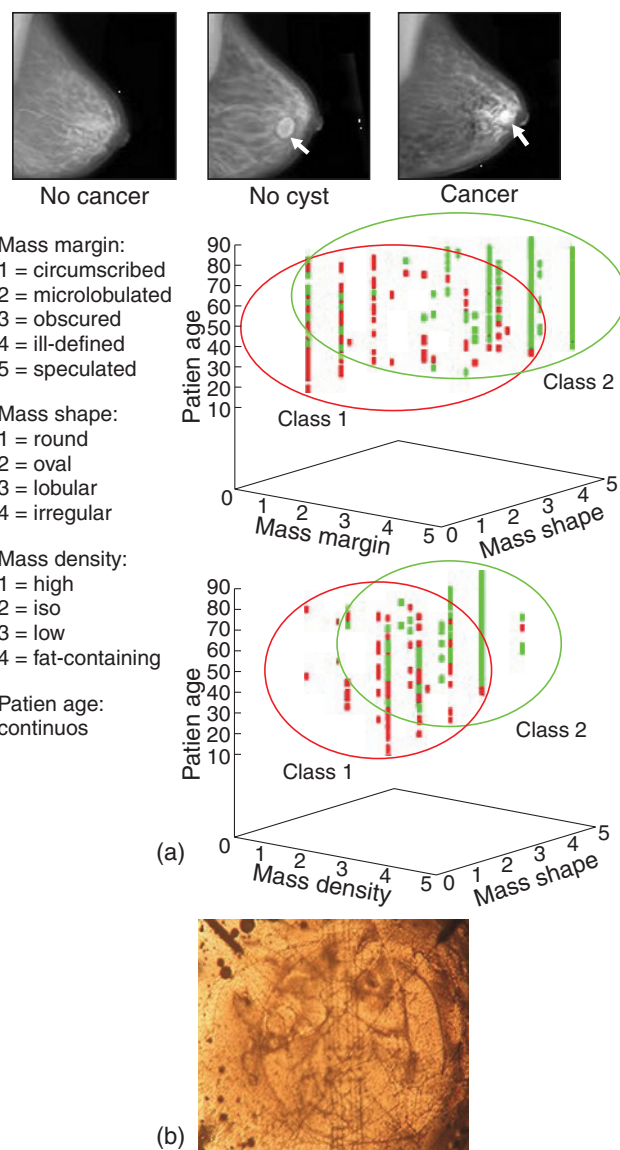


Fig. 1. (a) Mammographic Mass Dataset from the UCI [4] repository and photographs from [5] and (b) 0.05 wt% single-walled-carbon-nanotube / liquid crystal sample.

I/V response are potential candidates for EiM devices. The EA implemented in experiments, differential evolution (DE), is derivative-free, iterative and population-based. Its task is to modify the SWCNT/LC samples' state, maximising the difference between output currents produced by the material under the influence of input voltages representing benign and malignant data. It was observed that optimum solutions, i.e. classifiers with maximum accuracy, were a combination of optimal electric field and SWCNT network morphology, both produced by DE during training. Comparing the EiM and NN approaches shows that for similar classifier accuracy, less training data is

needed when the former is used. In addition, the SWCNT/LC diagnostics were marginally better than radiologists, but not as good as fellowship trained practitioner [9].

This work demonstrates the potential to replace traditional artificial machines, such as neural networks, with nanomaterials to solve complex computational problems. A persistent issue with the computation's accuracy was observed, which is common in the analogue computing case. This is a problem which can be addressed by improving the quality of the hardware used and the training algorithm's efficiency.

References

- [1] K.P. Murphy, *Machine Learning: A Probabilistic Perspective*. The MIT Press (2012).
- [2] A. Thompson. *In Evolvable systems: from biology to hardware*, 390–405. Springer, 1996.
- [3] J. F. Miller, *et al.* *Proceedings. NASA/DoD Conference on*, 167–176. IEEE, (2002).
- [4] M. Lichman. UCI machine learning repository, 2013.
- [5] National Cancer Institute. (2015). <https://www.cancer.gov/types/breast/understanding-breast-changes>
- [6] F. Arce, *et al.*, *In Symposium Series on Computational Intelligence (SSCI)*, IEEE, 1–8 (2016).
- [7] P. Jeatrakul *et al.*, SNLP'09. *Eighth Int. Symposium on IEEE*, 111–115 (2009).
- [8] D. Volpati, *et al.*, *J. of Applied Physics*, **117**(12) 125303, (2015).
- [9] J. G. Elmore, *et al.*, *Radiology*, **253**3, 641–651, (2009).

Increasing nanowire diameters for solar cell applications

D. Paige Wilson¹, R. LaPierre^{1,2}

¹ Department of Engineering Physics, Centre for Emerging Device Technologies, McMaster University, Hamilton, ON, Canada, L8S 4L7

² ITMO University, Kronverkskiy pr. 49, St Petersburg 197101, Russia

Improving the overall device efficiency of a nanowire solar cell relies strongly on optimizing the cell parameters with respect to both the optical absorption and the electrical properties of the materials. Numerical simulations have shown that for GaAs nanowires a nanowire array pitch of 350 nm with a wire diameter of 180 nm optimizes the photocurrent [1]. However, increasing the diameter of a nanowire results in greater strain due to lattice mismatch when a III-V nanowire is grown on a Si substrate. This effect is particularly important above a critical diameter of 110 nm for GaAs [2].

We show through numerical computations that the 180 nm thicker nanowires produce a higher device efficiency compared to thinner nanowires of 100 nm in diameter with pitch optimized for best absorption. We do so using a combination of rigorous coupled wave analysis (RCWA) [3] and finite element method (FEM). We propose the use of reverse-tapered nanowire structures to maintain high absorption near the tip of the wire without compromising yield due to strain at the base.

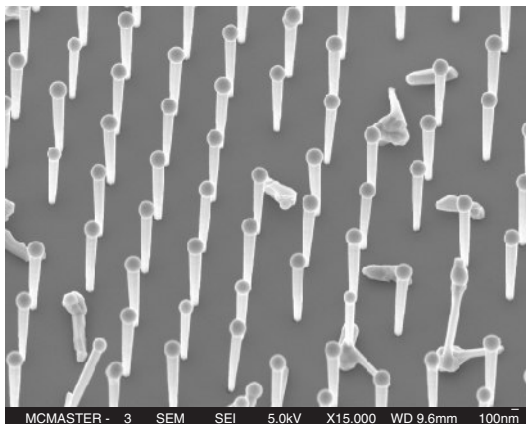


Fig. 1. SEM image of reverse tapered nanowires averaging 170 nm in diameter below the droplet and 111 nm at the top of the hole in the oxide layer.

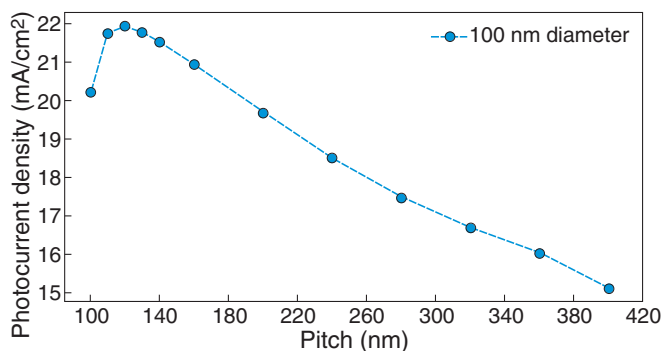


Fig. 2. Optimization of the photocurrent density with respect to the pitch of a nanowire array with diameters of 100 nm.

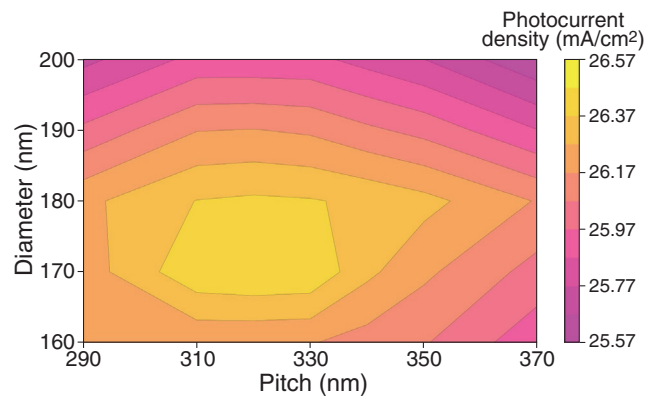


Fig. 3. Optimization of the photocurrent density with respect to pitch and diameter for wide diameter nanowires.

We show that these structures can be grown for self-assisted GaAs/GaP/Si nanowires by decreasing the V/III flux ratio during growth by molecular beam epitaxy (MBE) [4].

Acknowledgement

We gratefully acknowledge the work of K.W. Robertson of the University of Ottawa, Department of Physics for the development of a Python API for the S⁴ RCWA method.

References

- [1] Y. Hu, *et al*, *J. of Applied Physics*, **112**, 104311 (2012)
- [2] G. E. Cirlin, *et al*, *Physica Status Solidi (RRL)*, **3**, 112-114 (2009)
- [3] V. Liu, *et al*, *Computer Physics Communications*, **183**, 2233-2244 (2012)
- [4] P. Kuyanov, *et al*, *J. of Crystal Growth*, **462**, 29-34 (2017)

Model for growth modes of PA MBE GaN nanowires

Y. Berdnikov, N.V. Sibirev

ITMO University, Kronverkskii pr. 49, 197101, St Petersburg, Russia

GaN nanowires (NWs), grown via plasma-assisted molecular beam epitaxy (PA MBE), are considered as promising building blocks for novel optoelectronic devices because of their unique properties and low defect concentration in structures grown on silicon substrates [1]. Catalyst-free PA MBE NW form within the narrow window of experimental parameters, which can be estimated in the growth modeling.

Typically, the NWs grow from the N-rich vapor phase at substrate temperatures within the range of 730 to 830 °C. Lowering of the substrate temperature or increase of the III/V ratio leads to the formation of a 2D layer due to the coalescence of nanostructures. Contrary, no growth is usually observed at high temperatures or low Ga fluxes [2]. In this work, we present the model which gives the analytical expressions for the boundaries between the three growth modes (continuous layer, NWs, and absence of the growth).

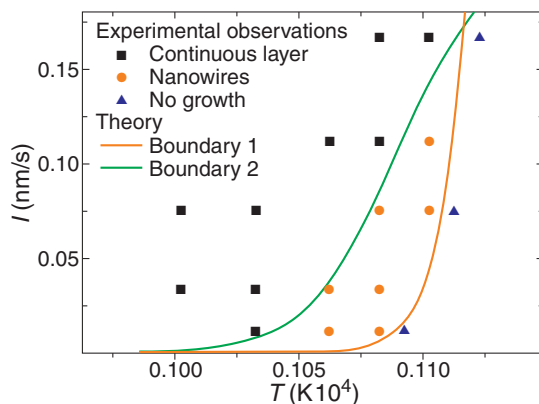
Within the model approach, the continuous 2D layer forms when during the growth the mean NW diameter exceeds the mean interwire distance, and their equality gives the boundary of this growth mode. No growth is predicted when the nucleation stage remains incomplete during the deposition time. At fixed N flux, the two boundary conditions delineate the region of NW growth in the Ga flux-growth temperature diagram. Figure 1 compares our theoretical results and experimental data of [2].

Acknowledgement

The authors acknowledge the financial support received from the Ministry of Education and Science of the Russian Federation under grant 14.587.21.0040.

References

- [1] V. Consonni, *Phys Status Solidi RRL*, **7**, 699 (2013).
- [2] S. Fernández-Garrido *et al*, *J. Appl. Phys.*, **106**, 126102 (2009).



Vapor-solid-solid growth mechanism of Au-catalyzed III-V nanowires

A.A. Koryakin^{1,2}, S.A. Kukushkin^{1,2,3}, N.V. Sibirev¹

¹ ITMO University, Kronverkskiy pr. 49, 197101, St Petersburg, Russia

² St Petersburg Academic University, Khlopina 8/3, 194021, St Petersburg, Russia

³ Institute of Problems of Mechanical Engineering RAS, 199178, St Petersburg, Russia

Semiconductor nanowires (NW) are promising candidates for the development of novel electronic and optoelectronic devices. At present, the epitaxial catalytic growth techniques (e.g. Au-catalytic) are most widely used to synthesize NW. In the pioneering work of Wagner and Ellis [1] devoted to the catalytic growth of Si whiskers (“microwires”), the vapor-liquid-solid (VLS) mechanism of crystal growth was proposed. According to this growth mechanism, there is a liquid droplet of catalyst seated on the crystal top and the crystal growth occurs at the temperature above the eutectic temperature for the given material system. In further studies [2,3], it has been found that the growth of Au-catalyzed NW of group III-V compounds (e.g. GaAs, InAs, InP, GaInAs) is possible both at the temperatures above and below the eutectic temperature. In these studies the eutectic temperature has been determined using the phase diagrams of gold and group III element. The binary phase diagrams can be used because the concentration of arsenic and phosphorus atoms solved in the catalyst is negligible (~1%). The vapor-solid-solid (VSS) mechanism has been proposed in the works [3,4] to explain the NW growth at the temperature below the eutectic point. According to the VSS mechanism, the catalyst is in the solid phase. However, considering only the equilibrium phase diagrams of binary systems, the role of the catalyst phase cannot be fully understood. First, the NW growth model must account for the kinetic factors that can influence the concentration of species diluted in catalyst particle. Second, it is necessary to consider the ternary phase diagrams instead of the binary phase diagrams. Third, if the radii of NW are small the influence of the catalyst surface on the NW nucleation rate can be significant (the Gibbs–Thompson effect). Thus, the issue on the phase of the catalyst during the semi-

conductor NW growth has not been elucidated as yet.

In this work, we present a theoretical study of the VSS growth mechanism of Au-catalyzed III-V NW and consider GaAs NW as an example of III-V system. The classical nucleation theory is used to calculate the nucleation rate of 2D-islands at catalyst-NW interface. The influence of the elastic stresses caused by the difference in the atomic densities of the catalyst and NW material on the solid nucleation rate is considered. The value of the elastic energy term in the Gibbs energy of coherent island formation is found to be larger than ~200–300 meV (Fig. 1) and comparable with the difference of the chemical potentials per the GaAs pair in catalyst and NW. We show that VSS growth mechanism is possible below the Au-Ga melting point 491.3° due to the grain boundary diffusion of As species along the catalyst-NW interface, whereas, the volume diffusion of As is negligible.

Acknowledgement

The reported study was funded by RFBR according to the research project No. 18-32-00559.

References

- [1] R.S. Wagner, W.C. Ellis *Appl. Phys. Lett.* **4**, 89 (1964)
- [2] B.J. Ohlsson *et al*, *Physica E* **13**, 1126 (2002)
- [3] P. Krogstrup *et al*, *Nano Lett.* **9**, 3689 (2009)
- [4] A.I. Persson *et al*, *Nature Mater* **3**, 677 (2004)
- [5] A.G. Khachaturyan *Theory of structural transformations in solids* New York: Dover (2008)

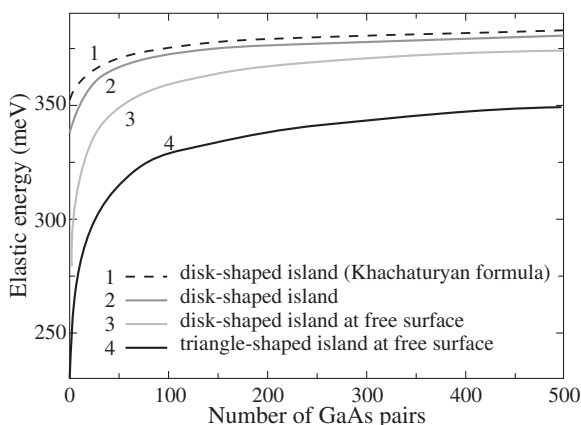


Fig. 1. The elastic energy per GaAs pair in the 2D island formed at the catalyst-NW interface versus the island size. The results of calculation by the finite-element method (solid lines) and the Khachaturyan formula [5] (dashed line) are shown for islands of different shape and position.

Au droplet stability in InAs nanowires growth

A.S. Sokolovskii, V.G. Dubrovskii

ITMO University, Kronverkskiy pr. 49, 197101, St Petersburg, Russia

Semiconductor nanowires (NWs) are predicted to be key components of future devices such as efficiency solar cells, lasers, functional nanoprobe and nanosensors. The Au-assisted vapor-liquid-solid (VLS) growth is the common approach to obtain high quality III-V NWs. A low solubility of most group V elements in Au-group III melts allows for minimising the reservoir effect [1]. This so-called reservoir effect has been investigated in detail experimentally and theoretically [2], and many efforts have been made to obtain sharp interfaces essential for device applications [1].

The InAs NWs with Au colloids were grown by chemical beam epitaxy on InAs(111)B substrates by VLS mechanism [3]. In the first experiments there were attempts for varying only one parameter: 1) temperature with fixed indium and arsenic fluxes; 2) In or As flux with fixed temperature. In the result, no swelling or shrinking of nanoparticles (NPs) wasn't observed, but with variation both fluxes and temperature, there is possible to observe NPs swelling or shrinking.

To understand kink formation mechanism, the following experiments were carried out: (1) InAs NWs were grown under fixed temperature 420 °C; (2) after the first 30 minutes of growth temperature was decreased to ° under As flux; (3) after the first 30 minutes of growth temperature was increased to 460 °C under In flux. In the first case, the contact angle of colloid NP on the NW top was 102 ° with In/Au ration equals 0.56. In the second case, cooling NWs under As flux leads to decreasing of In/Au ratio and also the contact angle. In the last case, heating of NWs under In flux causes an increase of both In/Au ratio and the contact angle of the NPs. The composition of NP In/Au was 4.88 and resulted first to the widening of top NW radius (approximately twice) and then in kinking.

We present model which describes region of acceptable values of NP contact angle for straight growth, and for kinking. Value of the contact angle below $\sim 95^\circ$ and greater than $\sim 129^\circ$ gives kinked NWs segment.

References

- [1] K.A. Dick, *et al*, *Nano Letters* **12**, 3200 (2012)
- [2] T.E. Clark, *et al*, *Nano Letters* **8**, 1246 (2008)
- [3] V. Zannier, *et al*, *Nano Letters* **18**, 167 (2018)

Author Index

- Akopian N., 15
Alkhalil F., 29
Amador N., 11, 25
Apollo M., 27
Arakawa Y., 12
Arbiol J., 28
Atkinson D., 29
Balgarkashi A., 28
Balog R., 6
Barbier C., 11
Baumberg J.J., 18
Belardini A., 20
Berdnikov Y., 47
Berthe M., 37
Bougerol C., 25
Bøggild P., 6
Camilli L., 6
Caroff P., 37
Cassidy A., 6
Cattoni A., 25
Centini M., 20
Chalermchai H., 25
Chechurin L., 32
Cirlin G.E., 15, 39
Collin S., 25
Dai X., 25
De Luca M., 14
Di Mario L., 33
Diaz-Alvarez A., 37
Dolbnya I.P., 18
Dubrovskii V.G., 17, 20, 28, 34, 36, 49
Dunin-Borkowski R.E., 37
Durand C., 11, 25
Durose K., 27
Ebert Ph., 37
Eisele H., 37
Eymery J., 11, 25
Feidenhans'l R., 22
Fontcuberta i Morral A., 9, 28, 29, 34
Francaviglia L., 28, 34
Friedl M., 28, 34
Güniat L., 28
Galan A., 29
Galeti H.V.A., 40
Gallant A.J., 29
Ghasemi M., 7, 36
Gholami E., 31
Glas F., 17, 38
Gobatoand Y.G., 40
Gogneau N., 11
Grandidier B., 37
Groves C., 44
Guñiat L., 34
Guan N., 11, 25
Guina M., 20, 35, 40
Hakkarainen T., 20, 35, 40
Harmand J.-C., 11, 17, 25, 38
Hornekær L., 6
Horrocks B., 42
Houlton A., 42
Johansson J., 7, 36
Joselevich E., 19
Julien F.H., 11, 25
Jørgensen J.H., 6
Kaliteevskii V., 32
Kapoor A., 11, 25
Kim W., 28, 34
Koivusalo E., 20, 35, 40
Korsunsky A.M., 18
Koryakin A.A., 48
Kotlyar K.P., 39
Kotsialos A., 44
Kukushkin S.A., 39, 48
LaPierre R.R., 13, 46
Largeau L., 11
Lashkani Z.M., 31
Leahu G., 20
Lefebvre I., 37
Leran J.-B., 34
Leshchenko E.D., 7, 36
Lu L., 11
Lupo D., 40
Madouri A., 11
Major J., 27
Mancini L., 11, 25
Martínez P.R., 42
Martelli F., 33
Marti-Sanchez S., 28
McIntyre P.C., 10
Mikulik D., 34
Morassi M., 11
Nestoklon M.O., 24
Nikitina E.V., 39
Nys J.P., 37
Oehler F., 25, 38
Osipov A.V., 39
Paige Wilson D., 46
Panciera F., 17
Patriarche G., 17, 37
Pearson C., 44
Peric N., 37
Petronijevic E., 20
Petty M.C., 44
Piazza V., 25
Pishchagin A., 38
Piton M.R., 20, 40
Plissard S.R., 37
Potts H., 34
Reznik R.R., 39
Roca i Cabarrocas P., 23
Rodrigues A.D., 40
Romanov A.E., 8
Rubini S., 33
Sadowski J.T., 6
Schnedler M., 37
Sibilia C., 20
Sibirev N.V., 47, 48
Sivan A.K., 33
Sokolovskii A.S., 49
Soshnikov I.P., 39
Souto S., 40
Stepniowski W., 27
Stoot A.C., 6
Stutz E., 34
Sui T., 18
Suomalainen S., 40
Tchernycheva M., 11, 25
Tersoff J., 6
Tormen M., 27
Tuñuicuoglu G., 34
Vissol-Gaudin E., 44
Vukajlovic-Plestina J., 34
Xu T., 37
Zeze D.A., 29, 44
Zhang H., 25
Zhao Q., 18
Zytkiewicz Z.R., 16

LIST OF PARTICIPANTS

Amador Nuño

C2N – Paris Sud University
nuno.amador@u-psud.fr

Andre Yamina

University Clermont Auvergne
yamina.andre@uca.fr

Apollo Manuel

University of Liverpool
Manuel.Apollo@liverpool.ac.uk

Arakawa Yasuhiko

University of Tokyo
arakawa@iis.u-tokyo.ac.jp

Arseneva Julia

ITMO University
yulia.ars@mail.ru

Atkinson Derek

Durham University
del.atkinson@durham.ac.uk

Berdnikov Yury

ITMO University
yury.berdnikov@corp.ifmo.ru

Chennupati Jagadish

Australian National University
Chennupati.Jagadish@anu.edu.au

Cirlin George

SBPAU, ITMO University
cirlin@beam.ioffe.ru

De Luca Marta

University of Basel
marta.deluca@unibas.ch

Dimakis Emmanouil

Institute of Ion Beam Physics
and Materials Research
e.dimakis@hzdr.de

Djoric Goran

ITMO University
gorandjoric2@gmail.com

Dubrovskii Vladimir

ITMO University
dubrovskii@mail.ioffe.ru

Ergun Ridvan

Durham University
ridvanergunn@gmail.com

Feidenhans'l Robert

EXFEL
robert.feidenhansl@xfel.eu

Foncuberta i Morral Anna

EPFL
anna.foncuberta-morral@epfl.ch

Friedl Martin

Ecole Polytechnique Fédérale
de Lausanne
martin.friedl@epfl.ch

Galan Alejandro

Durham University
alejandro.galan@durham.ac.uk

Gallant Andrew

Durham University
a.j.gallant@durham.ac.uk

Geelhaar Lutz

Paul-Drude-Institut
geelhaar@pdi-berlin.de

Gholami Ehsan

Innolume GmbH
ehgh@innolume.com

Gil Evelyne

University Clermont Auvergne
evelyne.gil@uca.fr

Glas Frank

University Paris Saclay
frank.glas@lpn.cnrs.fr

Hakkarainen Teemu

Tampere University of Technology
teemu.hakkarainen@tut.fi

Harmand Jean-Christophe

Université Paris-Sud,
Université Paris-Saclay
jean-christophe.harmand@c2n.upsaclay.fr

Huyet Guillaume

Institut de Physique de Nice
guillaume.huyet@inphyni.cnrs.fr

Jean Théo

ITMO University
theo.jean@etu.uca.fr

Johansson Jonas

Lund University
Jonas.Johansson@ftf.lth.se

Joselevich Ernesto

Weizmann Institute of Science
ernesto.joselevich@weizmann.ac.il

Kaliteevskaya Natalia

EU Marie Curie
Initial Training Network “INDEED”
natalia.kaliteevskaya@durham.ac.uk

Kaliteevskii Vasilii

Lappenranta University of Technology
vasilii.kaliteevskii@lut.fi

Kanjampurath Sivan Aswathi

IMM CNR
aswathi.sivan@artov.imm.cnr.it

Khan Sabbir Ahmed

Niels Bohr Institute,
University of Copenhagen
sabbir.khan@nbi.ku.dk

Khrebtov Artyom

ITMO University
khrebtovart@mail.ru

Kim Wonjong

EPFL
wonjong.kim@epfl.ch

King Jennifer

Durham University
jennifer.king@durham.ac.uk

Koivusalo Eero

Tampere University of Technology
eero.koivusalo@tut.fi

Koriakin Aleksandr

ITMO University
alexkorya@gmail.com

Korsunsky Alexander

Oxford University
alexander.korsunsky@eng.ox.ac.uk

LaPierre Ray

McMaster University
lapierr@mcmaster.ca

Leshchenko Egor

Lund University
egor.leshchenko@ftf.lth.se

Livshits Daniil

CEO Innolum GmbH
indeed@innolume.com

Markova Nadin

Organizing Committee
nadin.markova@gmail.com

McIntyre Paul

Stanford University
pcm1@stanford.edu

Nestoklon Michail

Ioffe Institute
nestoklon.coherent@mail.ioffe.ru

Nurmamytov Timur

CNR-IOM Institute of Materials
nurmamytov@iom.cnr.it
nurmamytovtimur@iom.cnr.it

Osipov Andrey

Institute of Problems
of Mechanical Engineering RAS
andrey.v.osipov@gmail.com

Peric Nemanja

CNRS
nemanjaperic678@gmail.com

Pishchagin Anton

Center for Nanoscience
and Nanotechnology, CNRS
apishch@gmail.com

Reznik Rodion

 ITMO University
 moment92@mail.ru
Riechert Henning

 Paul-Drude-Institut
 riechert@pdi-berlin.de
Rizzo Piton Marcelo

 Tampere University of Technology
 marcelo.rizzopiton@tut.fi
Roca Pere

 Ecole Polytechnique
 pere.roca@polytechnique.edu
Rojas Pablo

 Newcastle University
 pablo.rojas-martinez@ncl.ac.uk
Rylkova Marina

 ITMO University
 rylmarina@yandex.ru
Samsonenko Yury

 ITMO University
 yu.samsonenko@mail.ru
Sibirev Nickolay

 ITMO University
 NickSibirev@corp.ifmo.ru
Sibireva Elena

 Organizing Committee
 elenasibireva@gmail.com
Sokolov Daniil

 Technical Team
 Max-fill@mail.ru
Sokolova Zhanna

 Organizing Committee
 sokolova.zanna@mail.ru
Sokolovskii Andrei

 ITMO University
 sokolovskiy.a.s@niuitmo.ru
Tchernycheva Maria

 University Paris Sud
 maria.tchernycheva@u-psud.fr
Tertsoff Jerry

 IBM
 tertsoff@us.ibm.com
Ubyvovk Evgeny

 ITMO University
 ubyivovk@gmail.com
Viktorov Evgeny

 ITMO University
 evviktor@gmail.com
Vissol-Gaudin Eleonore

 Durham University
 eleonore.vissol-gaudin@durham.ac.uk
Wilson Debra Paige

 McMaster University
 wilsod1@mcmaster.ca
Zeze Dagou

 Durham University
 d.a.zeze@durham.ac.uk
Zhiglinsky Alexey

 ITMO University
 N/A
Zytkiewicz Zbignew

 Instytut Fizyki PAN
 zytkie@ifpan.edu.pl